


Review Article

Open Access



Micro-cylindrical/fibric electronic devices: materials, fabrication, health and environmental monitoring

Hongyang Wang^{1,2,#} , Hao Wu^{1,2,#}, Dong Ye^{1,2,*}, Chenyang Zhao^{1,2}, Qingshuang Wu^{1,2}, Sen Wang^{1,2}, Zhiwei Zhang^{1,2}, Mingtao Zeng^{1,2}, Hanghang Wei^{1,2}, YongAn Huang^{1,2,*}

¹State Key Laboratory of Intelligent Manufacturing Equipment and Technology, Huazhong University of Science and Technology, Wuhan 430074, Hubei, China.

²Flexible Electronics Research Center, Huazhong University of Science and Technology, Wuhan 430074, Hubei, China.

#Authors contributed equally.

* **Correspondence to:** Prof. YongAn Huang, Dr. Dong Ye, State Key Laboratory of Intelligent Manufacturing Equipment and Technology, Huazhong University of Science and Technology, No. 1037 Luoyu Street, Hongshan District, Wuhan 430074, Hubei, China. E-mail: yahuang@hust.edu.cn; yedong@hust.edu.cn

How to cite this article: Wang H, Wu H, Ye D, Zhao C, Wu Q, Wang S, Zhang Z, Zeng M, Wei H, Huang Y. Micro-cylindrical/fibric electronic devices: materials, fabrication, health and environmental monitoring. *Soft Sci* 2024;4:41. <https://dx.doi.org/10.20517/ss.2024.53>

Received: 21 Oct 2024 **First Decision:** 6 Nov 2024 **Revised:** 19 Nov 2024 **Accepted:** 22 Nov 2024 **Published:** 29 Nov 2024

Academic Editor: Seung Hwan Ko **Copy Editor:** Pei-Yun Wang **Production Editor:** Pei-Yun Wang

Abstract

Micro-cylindrical electronic devices represent a rapidly emerging class of electronics distinguished by their unique geometries and superior mechanical properties. These features enable a broad range of applications across fields such as wearable fibric devices, surgical robotics, and implantable medical devices. The choice of micro-cylindrical substrate materials is crucial in determining device performance, as their high curvature and excellent flexibility offer an ideal foundation for functional integration. This paper systematically reviews a wide array of substrate materials suitable for micro-cylindrical electronic devices, analyzing their differences and application potential in terms of mechanical stability, biocompatibility, and processability. The unique requirements of micro-cylindrical devices, specifically their flexibility, integrative capabilities, and lightweight nature, challenge conventional planar fabrication processes, which often fall short of meeting these demands. Thus, we further examine custom fabrication techniques tailored for micro-cylindrical electronics, assessing advantages, limitations, and specific applications of each approach. Additionally, we analyze the current application requirements and developmental progress of these devices across multiple fields. This review also outlines future directions in this field, focusing on enhancing fabrication precision, improving material compatibility and biocompatibility, and advancing integration and intelligent functionalities. With a comprehensive overview, this review aims to provide a valuable reference for



© The Author(s) 2024. **Open Access** This article is licensed under a Creative Commons Attribution 4.0 International License (<https://creativecommons.org/licenses/by/4.0/>), which permits unrestricted use, sharing, adaptation, distribution and reproduction in any medium or format, for any purpose, even commercially, as long as you give appropriate credit to the original author(s) and the source, provide a link to the Creative Commons license, and indicate if changes were made.



the research and development of micro-cylindrical electronic devices, promoting technological advancements and innovation in emerging applications.

Keywords: Micro-cylindrical electronics, fibric electronic systems, conformal manufacturing, wearable devices, surgical robotics, implantable medicine

INTRODUCTION

Micro-cylindrical and fibric electronic devices have garnered significant attention and application across various fields in recent years due to their unique geometric structures and superior mechanical properties. As shown in [Table 1](#), fibric-based devices exhibit distinct advantages over traditional film-based flexible electronics. These advantages include superior flexibility, breathability, and lightweight characteristics, making them well-suited for applications requiring extended wear and adaptability to complex surfaces. In addition, micro-cylindrical and fibric devices possess ultra-high curvature and high aspect ratios^[1], enhancing space utilization and enabling the integration of complex, fiber-based electronic systems within confined spaces. These devices typically exhibit exceptional flexibility and lightweight characteristics, allowing them to maintain stable performance across diverse conditions. In particular, fibric and micro-cylindrical materials are pivotal to the performance of micro-cylindrical and fibric electronic devices, directly influencing their functionality and application range. These substrates encompass a diverse array of types - including rigid, flexible, stretchable, and natural fibric materials - each suited to distinct structural designs and application demands. Rigid substrates, for instance, provide stable support ideal for applications such as sensors on the tips of surgical instruments^[2]. In contrast, flexible and stretchable substrates, prized for their deformability and stretchability, are well-suited for wearable and implantable medical devices^[3,4]. Natural fibers, known for their biocompatibility, degradability, and eco-friendly nature, further expand the range of applications in sustainable and bio-integrated electronics^[5]. Beyond mechanical resilience, these substrates must also meet the requirements of biocompatibility, electrical conductivity, and durability to ensure stable and reliable device performance in practical settings.

The unique geometrical features of micro-cylindrical substrates, characterized by their high curvature, aspect ratio, and flexibility, significantly influence the fabrication process of electronic devices. Conventional electrospinning techniques are effective for producing disordered fiber networks, often employed in the fabrication of thin-film sensors^[6,7]. However, they lack the capability to directly create patterned, functional structures on each individual micro-cylindrical or fibric surface. Conformal fabrication on micro-cylindrical surfaces requires not only addressing the mechanical adaptability of materials but also overcoming challenges such as high-precision patterning and multilayer integration on high curvature geometries^[8,9]. Based on these distinct characteristics, the manufacturing processes for micro-cylindrical electronics can be categorized into three main types, including additive, subtractive, and equivalent manners. Additive manufacturing builds complex three-dimensional structures onto micro-cylindrical substrates by sequentially stacking materials, utilizing techniques such as chemical coating^[10] and electroplating^[11], inkjet printing^[12], aerosol jet printing^[13], and electrohydrodynamic (EHD) printing^[14]. The key strength of additive manufacturing lies in its material compatibility and design flexibility, making it highly suitable for customized production^[15,16]. However, limitations remain in terms of precision and material stability, which require further optimization. Subtractive manufacturing, in contrast, achieves the desired structures through the removal of material, utilizing methods such as laser processing^[17], rotational exposure lithography^[18], and various etching techniques. Rotational lithography, for instance, allows for the generation of high-resolution patterns on curved surfaces by adopting high-precision masks. While subtractive manufacturing offers superior precision and repeatability, it tends to be more expensive and less efficient for complex designs. It is primarily employed in the fabrication of high-precision implantable medical devices^[19] and high-performance microsensors^[20]. The equivalent manufacturing process is

Table 1. Comparison between fibric-based devices and film-based devices

| Attribute | Fibric devices | Film devices |
|--|---|--|
| Flexibility | High flexibility; multi-degree-of-freedom bending with ultra-high curvature and high aspect ratio | Moderate flexibility; limited bending freedom |
| Stretchability | Easy to stretch; single-dimensional extension of surface elements (recoverable stretch > 100%) | Limited to stretch; low two-dimensional extension (typically < 5% tensile) |
| Breathability | Excellent breathability; compact fiber volume; mesh-like structure when woven | Poor breathability; low porosity compared to fibric devices |
| Thickness | Depending on textile thickness and design (typically > 100 μm) | Ultra-thin designs possible (typically < 50 μm) |
| Lightweight | Extremely lightweight; suitable for prolonged wearable use | Heavier than fibric devices; relatively high density |
| Integration of electronic components | Moderate integration; limited surface area; constrained high-density component integration | High integration; large surface area; supports diverse electronic components |
| Adaptability for large-area applications | Easy adaptability; compact structure; expansion without major performance or flexibility loss | Difficult adaptability; exponential component increase for large areas; increased manufacturing complexity |

primarily focused on transferring pre-fabricated shapes or structures onto micro-cylindrical substrates, ensuring the preservation of the material's integrity and properties. For instance, transfer printing and nanoimprinting techniques enable the precise replication of pre-fabricated thin films and nanoarray structures onto micro-cylindrical and fibric surfaces^[21,22]. While the equivalent manufacturing process offers advantages of high precision and material efficiency, its application in micro-cylindrical electronics remains challenged by issues such as alignment accuracy and structural integrity. In conclusion, the fabrication technologies for micro-cylindrical electronics are diverse, with each method tailored to specific application scenarios. The selection of a suitable manufacturing process must consider the trade-offs between precision, material compatibility, and cost-efficiency to optimize device performance for targeted applications.

Micro-cylindrical electronics have a broad range of applications across fields such as flexible wearable devices^[23], surgical robots^[24], and implantable medical devices^[25]. In the realm of wearable technology, fibric sensors enable the monitoring of physiological parameters and the acquisition of health data^[26,27], thanks to their flexible design that conforms to the human body^[28]. For instance, the integration of sensors and processing units within micro-cylindrical electronic devices allows for real-time monitoring of vital signs, including heart rate^[29], blood oxygen levels^[30], and body temperature^[5], thereby providing users with personalized health insights. In surgical robotics, the incorporation of sensors at the tips of surgical instruments (e.g., needles) facilitates real-time data feedback^[31], empowering surgeons to conduct more precise procedures. This capability not only reduces surgical risks but also enhances success rates, offering innovative solutions for complex, minimally invasive surgeries. The application of micro-cylindrical electronics is particularly extensive in the field of implantable medical devices, which include implantable stereo electroencephalogram (SEEG) electrodes^[32], deep brain stimulation (DBS) electrodes^[33], and biosensors^[34]. These devices, designed for prolonged use within living organisms, must meet stringent performance requirements, including favorable biocompatibility, long-term stability, miniaturization, and integration. Furthermore, as medical technology continues to advance, the potential applications of micro-cylindrical electronics, such as disease diagnosis^[35], drug delivery^[36] and rehabilitation therapy^[37], are increasingly highlighted. Thus, micro-cylindrical electronics not only enhance the functionality of traditional medical devices but also foster the development of novel medical solutions.

While micro-cylindrical electronic devices hold significant promise in both theoretical and practical applications, their material properties, fabrication processes and potential uses remain under-explored in existing literature. The absence of a systematic comparison and summary of micro-cylindrical substrate materials and conformal fabrication techniques has resulted in a lack of practical guidance, particularly for

emerging fields. To this end, this paper first reviews a range of commonly used materials for micro-cylindrical electronic devices, focusing on key properties such as suitability, conductivity, biocompatibility, and durability. Following this, a comprehensive overview of fabrication methods is provided, including conformal additive, subtractive, and equivalent manufacturing approaches. The respective advantages and limitations of each process will be adequately evaluated. Building on this analysis, the paper will further explore the typical applications of micro-cylindrical electronic devices across various fields, including wearable electronics, environmental monitoring, surgical robotics, implantable bioelectronics, and interventional magnetic resonance imaging (MRI) [Figure 1]. Additionally, this paper will examine the key technological bottlenecks that currently hinder the broader adoption of these devices, such as insufficient manufacturing precision, poor material compatibility, and high production costs. Proposed solutions to these challenges will be discussed, with the aim of advancing the practical application of micro-cylindrical electronics. In all, this paper seeks to provide a systematic overview of the fabrication processes and application scenarios for micro-cylindrical surface electronics, offering insights into their technical characteristics, applicable fields, and development trends. It is hoped that this work will serve as a valuable theoretical foundation and reference for future innovations in the field.

MATERIAL

In micro-cylindrical or fibric electronics and microsensors, the choice of substrate material is critical to device performance, comfort, and biocompatibility. Each type of substrate, whether rigid, flexible, stretchable, or natural fiber, offers distinct advantages in mechanical properties, electrical characteristics, and specific application scenarios. Rigid substrates are optimal for maintaining geometric stability, making them ideal for applications such as surgical instruments where precision and strength are paramount. Flexible substrates provide high mechanical tolerance and enhanced biocompatibility, addressing the need for durability and adaptability in wearable devices. With recent technological advancements, stretchable materials have further broadened the applications of flexible substrates, enabling smart sensors, soft robotics, and other devices in environments involving large deformations. In addition, natural fiber materials, due to their excellent biocompatibility and environmental sustainability, are increasingly selected for functional designs and eco-friendly electronics. While each substrate type shows significant potential in its respective domain, optimizing stability, performance, and long-term reliability remains essential for advancing future applications.

Rigid micro-cylindrical/fibric materials

Rigid micro-cylindrical substrates, such as stainless-steel pins, tungsten pins, and polyimide (PI) rods, are widely used as foundational materials for constructing micro-sensors, high-density electrodes, and other electronic devices, particularly in applications requiring precise localization. With stable mechanical properties, these substrates offer highly controllable geometries and structural strength, making them ideal for accurate signal acquisition and transmission in complex environments. This stability supports delicate operations such as deep tissue dissection and electrical monitoring^[46-48]. For instance, in tissue biopsies, multimodal sensor arrays integrated onto the surface of a rigid micro-cylindrical needle can simultaneously measure parameters such as tissue conductivity, pH, and glucose concentration^[2]. Rigid substrates are also commonly used in neural interfaces^[49] and minimally invasive surgical tools^[50]. These materials typically exhibit good chemical stability and durability, maintaining their mechanical and electrical properties even after extended use or repeated sterilizations.

Compared to flexible or stretchable substrates, rigid materials are more suitable for applications demanding a wider temperature tolerance and greater penetration into biological tissues^[32]. However, rigid micro-cylindrical substrates face limitations in biological applications, including reduced compatibility and

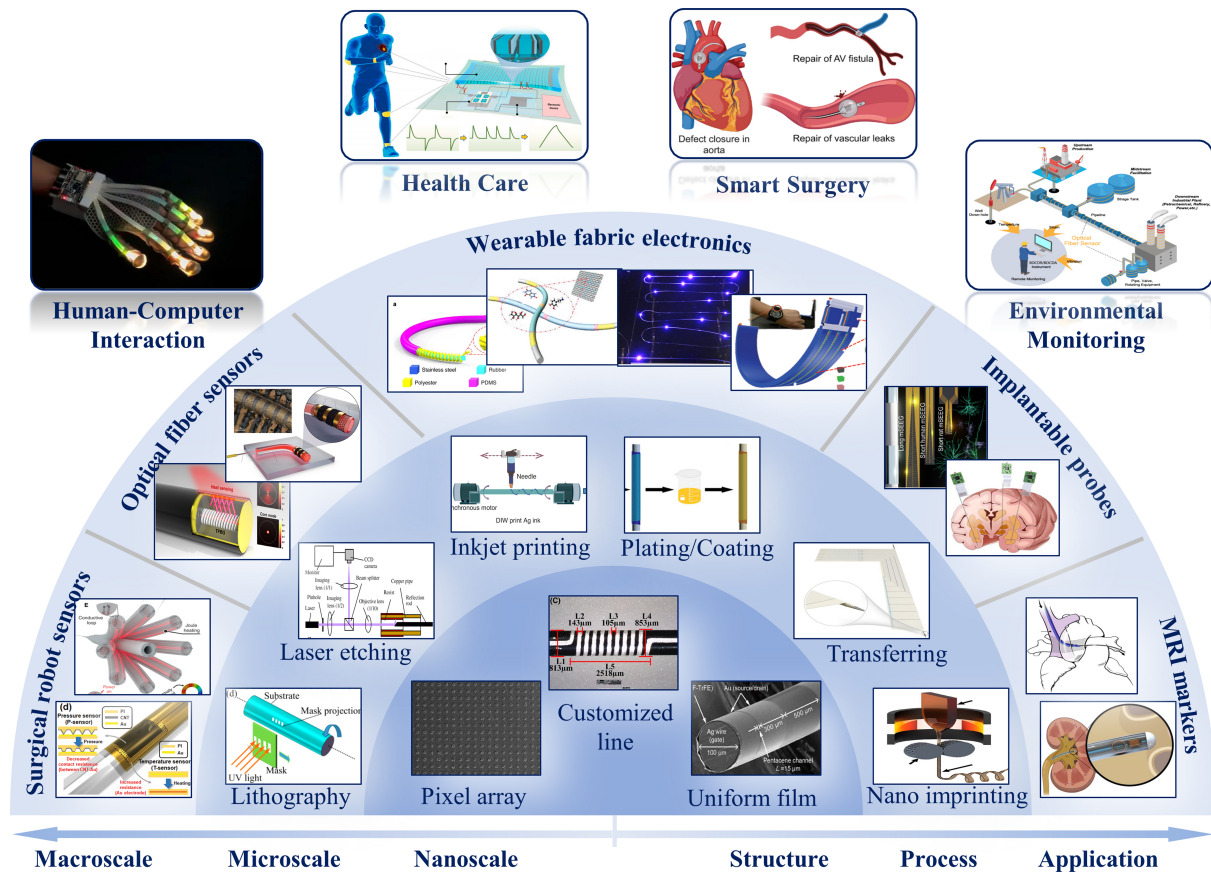


Figure 1. Fabrications and applications of micro-cylindrical and fibric electronic devices. Diverse structure (e.g., pixel array), Reproduced with permission^[38]. Copyright 2020, Springer Nature, customized line, Reproduced with permission^[39]. Copyright 2024, John Wiley and Sons, and uniform film, Reproduced with permission^[20]. Copyright 2020, American Association for the Advancement of Science, various process technologies (e.g., lithography), Reproduced with permission^[40]. Copyright 2018, MDPI, laser etching, Reproduced with permission^[17]. Copyright 2014, IOP Publishing on behalf of the Japan Society of Applied Physics, inkjet printing, Reproduced with permission^[29]. Copyright 2023, Springer Nature, plating/coating, Reproduced with permission^[41]. Copyright 2022, Sage Publications, transferring^[32]. Copyright 2024, Springer Nature, and nanoimprinting, Reproduced with permission^[38]. Copyright 2020, Springer Nature, a broad range of applications (e.g., surgical robot sensors), Reproduced with permission^[24]. Copyright 2024, John Wiley and Sons, optical fiber sensors, Reproduced with permission^[42]. Copyright 2023, John Wiley and Sons, wearable fabric electronics, Reproduced with permission^[43]. Copyright 2019, John Wiley and Sons, implantable probes^[32,44]. Copyright 2024, Springer Nature, Reproduced with permission. Copyright 2024, Springer Nature, and MRI markers, Reproduced with permission^[45]. Copyright 2022, John Wiley and Sons, and kinds of sceneries (e.g., human-computer interaction, health care, smart surgery and environment monitoring).

adaptability with soft tissues, which may lead to increased stress on surrounding tissues and influence long-term biocompatibility. Therefore, optimized design is essential for applications involving tissue contact, such as incorporating passivation layers near electrodes or employing surface modifications to minimize friction and tissue damage^[51]. In summary, while rigid substrates offer exceptional mechanical and electrical properties, balancing these benefits with biocompatibility is crucial to maximizing their potential in minimally invasive and biomedical electronic applications.

Flexible and stretchable micro-cylindrical/fibric materials

Flexible micro-cylindrical and fibric substrate materials, including metal wires, composite polymer fibers, and polymer optical fibers (POFs), are widely utilized in wearable electronics and flexible sensors due to their soft, lightweight properties^[52-54]. Compared to traditional rigid substrates, flexible fibric substrates offer superior mechanical tolerance during deformation and can maintain both structural and functional stability

through repeated bending cycles^[55]. For instance, by depositing silver nanoparticles (AgNPs) onto the surface of flexible fibers, high-sensitivity pressure sensors can achieve long-term durability exceeding 5,000 cycles^[56]. Additionally, flexible fibric structures are breathable and biocompatible, making them well-suited for skin-contact applications such as wearable electronics and biosensors^[57,58]. In the field of energy storage, flexible fibric substrates also find a broad range of applications. By integrating poly(terephthaloyl terephthalamide) (PPTA) fibers with carbon nanotubes (CNTs) or conductive polymers, flexible supercapacitor electrodes with high mechanical strength and thermal resistance can be produced, ensuring excellent electrochemical stability even under elevated temperatures^[59]. The porous nature and high specific surface area of flexible micro-cylindrical substrates further enhance their performance in energy storage and sensing applications. The rough fiber structure on these substrates can accommodate more active materials, thereby improving the energy and power density of the device^[3]. With ongoing advancements in material science and fabrication processes, flexible micro-cylindrical and fibric substrates are poised to play a crucial role in the development of next-generation wearable devices and smart electronic products.

Stretchable micro-cylindrical and fibric substrate materials represent an advanced extension of flexible materials, specifically designed to maintain stable performance under large deformations or extreme tensile conditions. Unlike flexible materials, stretchable materials can endure substantial mechanical strains (even over 100% elongation)^[60]. These materials are typically engineered using highly elastic polymers, which not only provide significant elongation but also retain strong mechanical and electrical properties during stretching^[41,61]. For example, conductive polymer materials in stretchable sensors enable continuous operation even in high-strain environments^[62,63]. Additionally, hydrogels, with their unique elasticity, stretchability, and excellent biocompatibility, demonstrate great potential for flexible sensors and biomedical devices^[4,64-66]. As a result, stretchable materials not only improve the comfort of wearable devices but also expand their potential for use in high-strain environments, such as smart sensors and soft robotics.

Natural micro-cylindrical/fibric materials

Natural fibric materials offer excellent environmental sustainability and biodegradability, and their structures can be adjusted both physically and chemically to meet the specific requirements of various applications^[67,68]. Among these, silk, a natural fiber, is particularly notable for its exceptional mechanical strength, biocompatibility, and degradability. However, natural silk is inherently non-conductive, necessitating the coating with other materials, such as CNTs, to enhance its functionality^[68]. Other natural fibers, such as cotton, have also garnered significant attention in the field of flexible electronics. By assembling gold nanoparticles (AuNPs) onto cotton fibers, their electrical conductivity can be substantially enhanced, improving their electrical interaction with enzymes and enabling their use in biofuel cells^[69].

Overall, natural fibric substrates are valued for their outstanding mechanical and chemical properties, as well as their biocompatibility, making them an attractive choice for the development of functionalized designs and environmentally friendly electronic materials^[5,70]. However, the mechanical properties of natural fibers are sensitive to variations in humidity and temperature, and they may experience degradation over prolonged use, which could compromise their reliability and stability in long-term applications. Despite these challenges, the limitations of natural fibers can be effectively mitigated through advanced processing techniques and optimized composite structures. These advancements facilitate the widespread adoption of natural fibers in flexible electronics, smart textiles, and biomedical applications^[71].

FABRICATION

Driven by the multifunctionality and wide applications of micro-cylindrical electronic devices, substantial research has been conducted on manufacturing technologies for these devices. There is increasing interest

on manufacturing strategies to transition from planar substrates to high-curvature micro-cylindrical substrates. Due to the high curvature, high aspect ratio, and flexibility of micro-cylindrical surfaces, researchers have developed various techniques, including conformal lithography, laser processing, inkjet printing, coating and plating technologies, flexible electronics transfer, and nanoimprinting. These techniques enable the fabrication of different components, such as pixels, wires, and films, on high-curvature micro-cylindrical surfaces, combining them into functional structures for active stimulation, passive sensing, and insulating encapsulation. [Table 2](#) summarizes the pros and cons of each method, highlighting their suitability for specific applications and detailing the comparative advantages and limitations of each technique. Based on material and structural formation, micro-cylindrical-specific manufacturing technologies can be further categorized into three types: precision material subtractive techniques based on exposure etching and high-energy laser ablation, enabling ultra-high-resolution microstructure formation; additive deposition techniques through dipping, coating, physical/chemical plating, and 3D printing, suitable for large-scale conformal manufacturing; and 3D structure equivalent technologies using transfer and imprinting, offering advantages for efficient production.

Subtractive technologies for high-resolution microstructures

Photolithography^[9,20,72-74] and laser processing^[75-77] are the common subtractive techniques to achieve microstructure fabrication and patterning, for their ability to precisely manipulate light or laser beams to create high-resolution features on substrates, particularly in complex applications such as high-curvature micro-cylindrical surfaces. They share a common focus on accuracy and high spatial resolution, and can be adapted for diverse material systems by fine-tuning process parameters such as energy intensity, wavelength, and beam focus. As key enablers of precision patterning and functionalization, these processes are vital for manufacturing intricate electronic structures on high-curvature surfaces.

Conformal lithography by selective exposure

Photolithography is a viable strategy for fabricating ultra-high-resolution features, and adapting traditional planar photolithography to high-curvature micro-cylindrical surfaces is of significance and challenge. The key to micro-cylindrical surface photolithography lies in minimizing the patterning mapping errors on high-curvature surfaces^[9,20,72,73]. Various photolithography schemes have been developed for both mask-based and mask-less photolithography, enabling selective exposure and removal of photosensitive materials to meet the patterning requirements of high-curvature micro-cylindrical objects.

Mask-based photolithography utilizes high-precision masks and optimized exposure setups to reduce exposure mapping errors on micro-cylindrical surfaces, leveraging rotational exposure systems for effective lithography. Some studies focus on improving exposure equipment and strategies to adapt to micro-cylindrical objects. For example, Yang *et al.*^[40] used a cylindrical projection lithography system to pattern the surface of a 1 mm diameter capillary substrate, developing rotational exposure equipment to scan the mask projection along and around the substrate [[Figure 2A](#)]. Similarly, Toshiyuki *et al.* used rotary scanning projection lithography on a 2.5 mm diameter substrate with an edge-width slit mask to project high-performance imaging^[78], scanning a spiral pattern on the substrate [[Figure 2B](#)]. Other studies have taken advantage of the conformal properties of flexible masks and substrates. Doll *et al.* patterned an 8 mm diameter small cylindrical surface using a chromium-plated polymer flexible mask^[79], reducing exposure errors through the conformal characteristics of the elastic polymer with the substrate [[Figure 2C](#)]. Park *et al.* successfully fabricated high aspect ratio copper structures on a 20 mm diameter micro-cylindrical object using a flexible SU-8 lithographic mask, incorporating a planar micro-slit mask to prevent undesirable exposure from soft lithography^[80] [[Figure 2D](#)]. High-resolution and conformal mask design and fabrication were applied to minimize mapping errors.

Table 2. Pros and cons of different fabrication techniques and their application areas

| Fabrication techniques | | Pros | Cons | Areas |
|--------------------------|-----------------------------------|---|--|--|
| Subtractive technologies | Conformal lithography | Ultra-high resolution microstructure formation; mature process parameter configurations | Limited processing size; projection errors on micro-cylindrical surfaces | High-density micro-nano devices; moderate fiber diameter |
| | Laser processing | Non-contact and easy manufacturing | Significant heat generation; substrate prone to damage | Micro-cylindrical substrates with high thermal stability |
| Additive technologies | Conformal printing | Controllable pattern resolution; adaptable to various substrates | Low manufacturing efficiency due to nozzle path tracking | Multifunctional multi-material micro-nano devices; suitable for ultra-fine fibers |
| | Plating and coating | Uniform thin film formation; suitable for large-scale manufacturing | Challenging to achieve high-resolution processing | Thin film manufacturing on long substrates; applicable to ultra-fine fibers |
| Equivalent technologies | Transferring flexible electronics | Mature planar processes; easily integrates complex electronic structures | High curvature surfaces induce significant bending stress, leading to structural damage | Integration of complex, multifunctional multilayer electronic devices; moderate fiber diameter |
| | Nanoimprinting | High-fidelity replication of 3D micro-nano structures; suitable for mass production | High manufacturing cost; limited mold precision; less adaptable to high-curvature substrates | 3D structured micro-nano functional devices; moderate fiber diameter |

To further reduce the projection errors of masks on micro-cylindrical surfaces, researchers have developed mask-less lithography techniques, using high-resolution beams to directly pattern micro-structures with the aid of rotational exposure systems. Tamaki *et al.* performed mask-less lithography on the surface of a 360 μm diameter microprobe, utilizing high-resolution beam path planning for patterning^[19] [Figure 2E]. Yang *et al.* employed a custom-built rotating ultraviolet (UV) lithography system to plan path on the substrate^[81], achieving a patterned micro-cylindrical structure of 330 μm [Figure 2F]. Hwang *et al.* integrated various electronic components on a 150 \times 150 μm square microfiber, using a mask-less aligner for patterning metal electrodes^[18]. These studies typically require both the beam and the motion platform to maintain high precision for minimizing mapping errors.

Laser processing for direct and controlled ablation

Laser processing technology utilizes high-energy laser beams to ablate complex patterns on the micro-cylindrical surface through precise path planning. This technique can be categorized based on its application to either the internal or external surfaces of cylindrical objects^[75-77].

For laser ablation processing on the outer surface, Haga *et al.* designed the structure of a hydraulically actuated bending catheter, using femtosecond laser processing to treat a super-elastic nitinol tube^[82] [Figure 3A]. These components feature multiple ring-arranged structures, with each ring having an outer diameter of 0.8 mm and an inner diameter of 0.75 mm. The innovation of this process lies in the use of a laser ablation system, which allows precise machining of the super-elastic alloy on micro-cylindrical surfaces while coating the thin-walled silicone rubber tube to enhance its functionality and durability. For processing inside the tube, Horiuchi *et al.* used laser scanning technology to create complex patterns within small-diameter tubes with 423 μm in diameter^[17] [Figure 3B]. They utilized a 408 nm wavelength semiconductor violet laser to project high-density multi-helix patterns onto the inner surface of the tube, by passing it through a pinhole and precision imaging optical system. This technique's innovation lies in its capability to achieve submicron manufacturing precision within extremely small-diameter tubes, while combining photolithography and chemical etching to achieve the desired inner surface characteristics.

The common features of these two laser processing technologies include high-precision manufacturing, suitability for small-diameter tubes, the ability to apply complex patterns precisely, and meeting functional

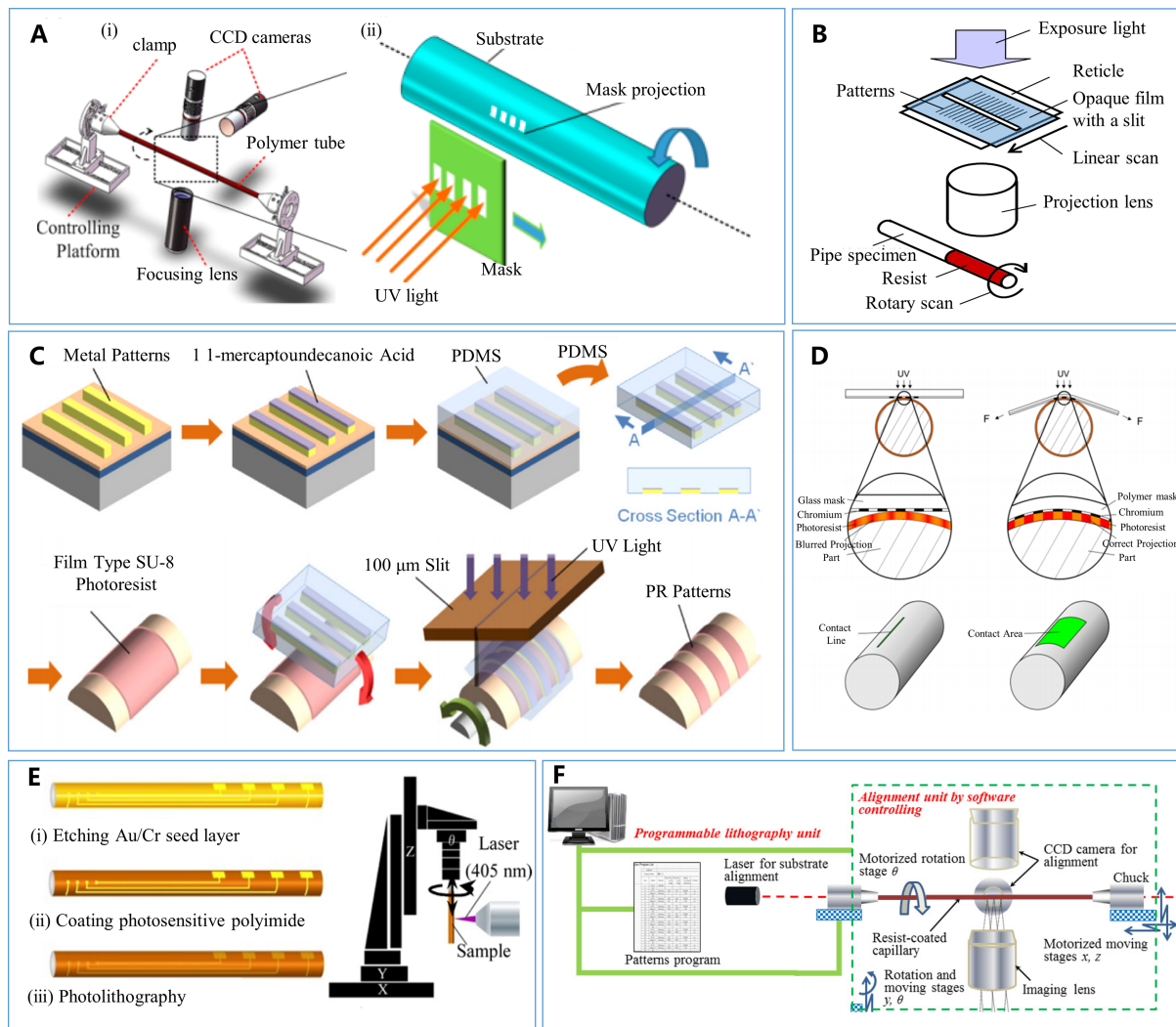


Figure 2. Photolithography-based fabrication methods on micro-cylindrical surfaces. (A) Cylindrical direct projection lithography. Reproduced with permission^[40]. Copyright 2018, MDPI; (B) Variable-width slit mask-assisted lithography^[78]. Copyright 2015, SPST; (C) Chromium-coated polymer flexible mask-assisted lithography. Reproduced with permission^[79]. Copyright 2020, IOP Publishing Ltd; (D) Combination of flexible SU-8 photolithographic mask and planar slit mask lithography. Reproduced with permission^[80]. Copyright 2011, Elsevier; (E) Mask-less lithography using high-resolution light beams. Reproduced with permission^[19]. Copyright 2017, John Wiley and Sons; (F) Programmable improved UV lithography system^[81]. Copyright 2013, WORLD SCIENTIFIC PUBL CO PTE LTD. UV: Ultraviolet.

requirements for both the outer and inner surfaces through different processing methods.

Additive technologies for wide adaptability and multifunctionality

Inkjet printing^[16,83] and coating/plating^[9,10,56,84] technologies are commonly used additive manufacturing techniques, both focusing on material deposition to create functional structures on substrates. These methods are highly adaptable for producing uniform coatings or patterned features on high-curvature micro-cylindrical surfaces. They are essential for manufacturing advanced electronics on micro-cylindrical surfaces, providing high adaptability to various material types and substrate geometries while maintaining functional integrity.

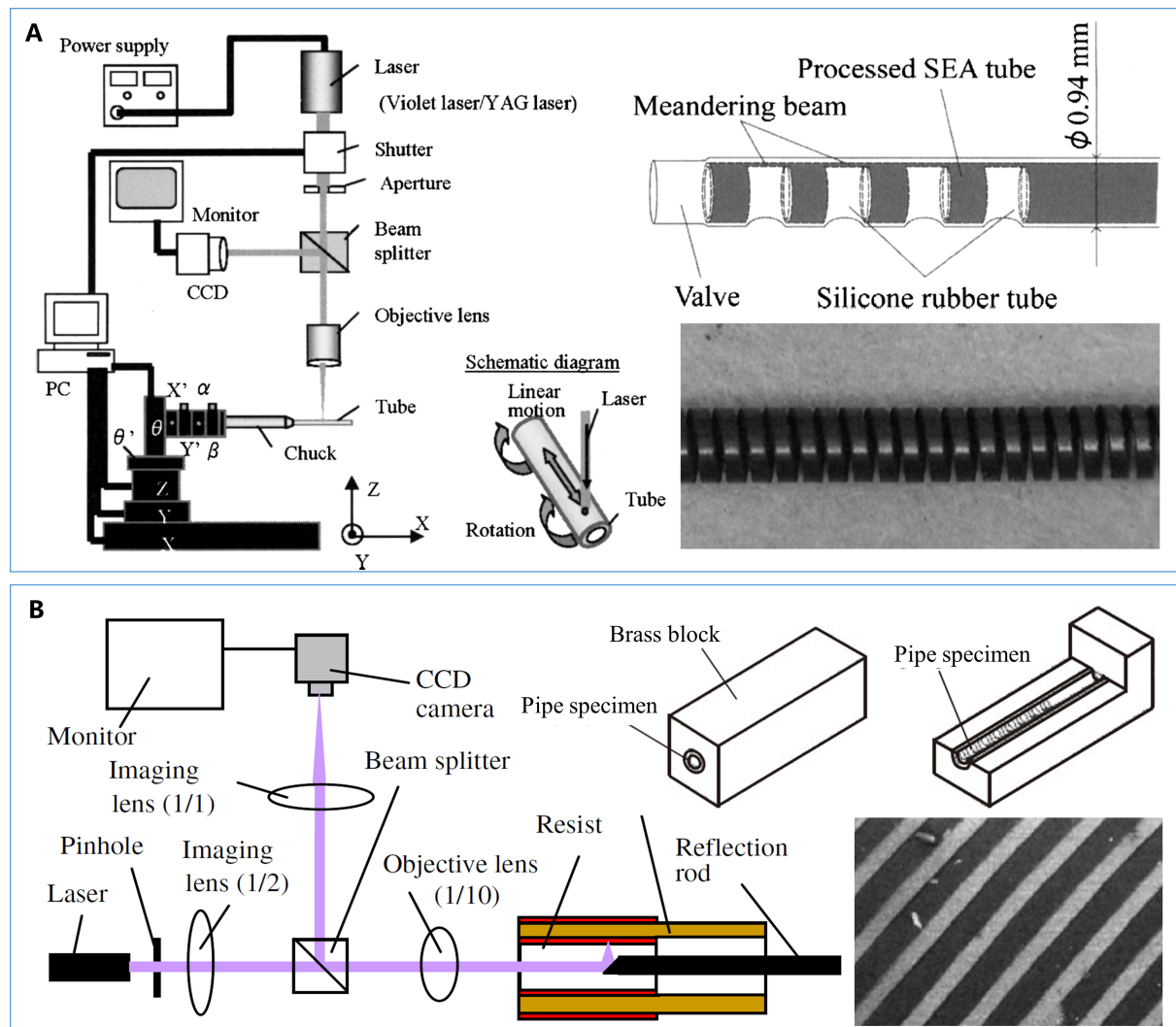


Figure 3. Laser processing fabrication technology on the inner and outer surfaces of micro-cylindrical objects. (A) Customizable path processing on the outer surface of a micro-cylindrical object via laser ablation. Reproduced with permission^[82]. Copyright 2011, John Wiley and Sons; (B) Laser scanning processing on the inner surface of a micro-cylindrical object. Reproduced with permission^[17]. Copyright 2014, IOP Publishing on behalf of the Japan Society of Applied Physics.

Conformal printing for non-contact deposition

Inkjet printing is a non-contact additive manufacturing technique that, by planning the relative movement path of the nozzle and the substrate, enables the fabrication of patterned structures on high-curvature surfaces^[12,83,85,86]. Based on the principle of ink deposition, inkjet printing can be divided into extrusion printing^[87,88], aerosol jet printing^[13], EHD printing^[14], and electrospinning^[89]. Table 3 presents a comparison of different types of inkjet printing techniques.

For extrusion printing technology, it is the most commonly used inkjet printing method, utilizing substrate rotation equipment to achieve micro-cylindrical printing. Li *et al.* proposed the fabrication of one-dimensional stretchable fiber-shaped electronic devices through inkjet printing technology, with a minimum diameter of $500 \mu\text{m}$ ^[15] [Figure 4A]. They developed precision rotary inkjet printing equipment and surface chemical modification processes, achieving wire structures with a line width of approximately $130 \mu\text{m}$ and customizable micro/nanofabrication. Zhang *et al.* also used direct ink writing technology to

Table 3. Comparison of different types of inkjet printing techniques

| Types | Materials | Substrates | Diameter | Accuracy | Ref. |
|----------------------|------------------------------|------------------------------|-------------------|-------------------------|------|
| Inkjet printing | Ag ink (28 cP) | PU fiber substrate | 500 μm | 133 μm | [15] |
| Aerosol jet printing | AgNPs flake ink | PTFE | 2.248 mm | 250 μm | [13] |
| EHD printing | Ag-PCL mixed ink | Glass and silicon substrates | 4 mm | $8 \pm 0.4 \mu\text{m}$ | [90] |
| | PCL | Glass microtubes | 1-10 mm | 80 μm | [14] |
| Electrospinning | Ultrafine polyaniline fibres | - | - | < 5 μm | [89] |

PU: Polyurethane; AgNPs: silver nanoparticles; PTFE: polytetrafluoroethylene; EHD: electrohydrodynamic; PCL: polycaprolactone.

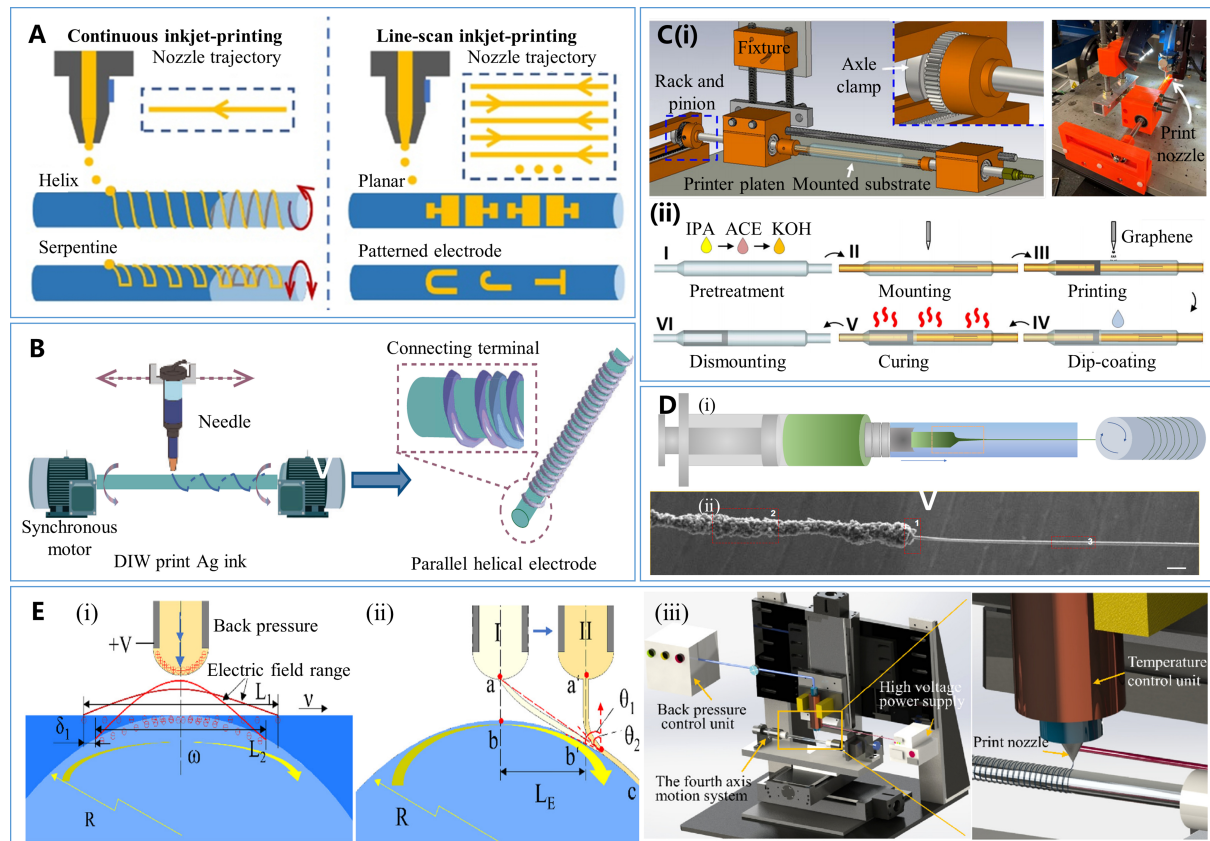


Figure 4. Inkjet printing fabrication technology on micro-cylindrical surfaces. (A) Extrusion-based inkjet printing for customizable path fabrication. Reproduced with permission^[15]. Copyright 2023, Elsevier; (B) Spiral ink writing on micro-cylindrical surfaces. Reproduced with permission^[29]. Copyright 2023, Springer Nature; (C) (i) Schematic illustration of the LAJ printing process. (ii) Step-by-step fabrication workflow of a graphene sensor on a catheterized balloon. Reproduced with permission^[91]. Copyright 2024, Springer Nature; (D) Microscale printing based on electric field-driven jet. Reproduced with permission^[89]. Copyright 2022, Springer Nature; (E) Electric field-driven printing with a pre-set eccentricity strategy. Reproduced with permission^[14]. Copyright 2023, Elsevier. LAJ: Lathe-based aerosol jet.

fabricate flexible capacitive strain sensors on the surface of fibers with diameters ranging from 0.5 to 1.5 mm, and demonstrated excellent sensing performance^[29] [Figure 4B].

To improve the quality of ink deposition, modifications have been made to both the ink materials and deposition methods. Aerosol jet printing involves spraying the material in the form of aerosol microdroplets, which can enhance the printing resolution. For example, by leveraging lathe-based aerosol jet (LAJ) printing in combination with a rotatable substrate platform, flexible multilayer CNT transistors

and graphene-based sensors for temperature and inflation monitoring have been successfully fabricated on the surfaces of airbag catheters^[91] [Figure 4C]. In addition, Jordan *et al.* used aerosol jet printing to fabricate inductively coupled radio frequency coil markers on a polymer catheter with a diameter of approximately 2 mm, achieving a printed wire width of about 250 μm ^[13].

EHD printing and electrospinning techniques involve applying a high-voltage electric field between the nozzle and the substrate. The high electric field force pulls the ink out of the nozzle, forming a submicron-scale jet, which improves ink deposition resolution. Zhang *et al.* proposed a microscale printing technique based on electric field-driven jetting, which only requires a single potential at the nozzle electrode to form the strong electric field, thereby eliminating the shape limitation of the substrate^[90]. Fang *et al.* used electrospinning to prepare ultrafine polyaniline fibers with diameters below 5 μm , achieving excellent performance^[89] [Figure 4D]. Peng *et al.* used electric field-driven printing to fabricate thin-walled tubular mesh structures on substrates with diameters ranging from 4 to 8 mm, proposing a pre-set eccentric strategy to mitigate the uneven electric field distribution caused by high-curvature substrates^[14] [Figure 4E].

The aforementioned techniques utilize substrate rotation equipment to adapt traditional printing methods to high-curvature micro-cylindrical surfaces, improving the positioning accuracy of the nozzle and the substrate to achieve higher-precision patterned structures.

Plating and coating for layer deposition

The coating/plating process is an important technique to prepare uniform and dense films around on the surface of micro-cylindrical substrates, aimed at altering surface properties or imparting new functionalities^[9,10,56,84]. The elongated characteristics of micro-cylindrical objects make them well-suited for coating and plating processes, which can be categorized into physical coating techniques and chemical plating techniques based on the principle of material deposition^[11,18,92-94]. Table 4 provides a comparison of different types of coating/plating techniques.

Physical coating techniques utilize mechanical, thermal, or other physical methods to apply functional materials uniformly to the substrate surface. For example, Ham *et al.* used a direct dip-coating method to uniformly coat organic ferroelectric poly(vinylidene fluoride-trifluoroethylene) [P(VDF-TrFE)] material on a 100 μm diameter Ag wire, fabricating substrate-free ferroelectric organic transistors that achieve one-dimensional artificial multi-synapse functions^[20] [Figure 5A]. Lee *et al.* proposed a suspended shear dip-coating method to attach deformable semi-solid liquid metal particles (LMP) onto fiber surfaces, significantly enhancing the coating's durability, conductivity, stretchability, and biocompatibility^[95] [Figure 5B].

Compared to physical coating techniques, chemical plating involves chemical reactions during the process, such as electrochemical, redox, and *in-situ* chemical reduction mechanisms. Woo *et al.* incorporated hydrogel ionic diode systems onto fiber electrodes through electroplating and spin-coating, where the uniform coating ensured device stability^[96] [Figure 5C]. Huang *et al.* synthesized conductive composite fibers with AgNPs conductive sheaths via *in-situ* chemical reduction, embedding AgNPs within the core fibers to form a novel sensing mechanism, leading to the development of an AgNPs/double covered yarn (DCY) composite yarn strain sensor^[41] [Figure 5D]. Liao *et al.* synthesized textile-like V6O13 nanomaterials onto aligned CNT fibers using a solution-redox method to fabricate self-charging fiber electrodes, effectively mitigating active material detachment and cracking during deformation^[97] [Figure 5E].

Table 4. Comparison of different types of coating/plating techniques

| Types | Materials | Substrates | Diameter | Accuracy | Ref. |
|-----------------------------------|--------------|------------------|----------------------------|-----------------------------------|------|
| Direct dipping coating | P(VDF-TrFE) | Ag wire | 100 μm | -608 nm | [20] |
| Suspended shear dipping | PaLMs; CaLMs | Fiber | 20 μm | - | [95] |
| Electrochemical plating | Zn/Ti | Fiber electrodes | 500 μm | 8 μm / 3 μm | [96] |
| <i>In-situ</i> chemical reduction | AgNPs | DCY | 639 \pm 19 μm | 15-19 μm | [41] |
| Solution redox | V6O13 | CNT | - | - | [97] |

P(VDF-TrFE): Poly(vinylidene fluoride-trifluoroethylene); LMPs: liquid metal particles; AgNPs: silver nanoparticles; DCY: double covered yarn; CNT: carbon nanotube.

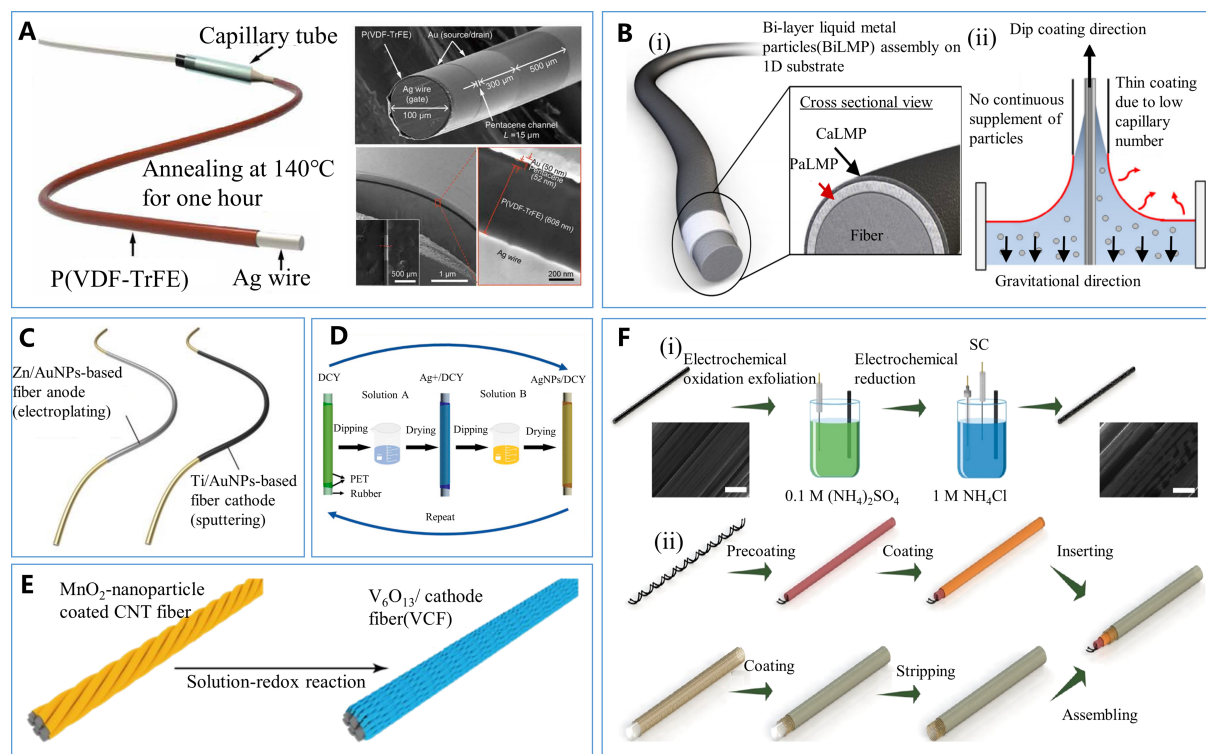


Figure 5. Fabrications of coating/plating technologies on micro-cylindrical surfaces. (A) Direct dip-coating method. Reproduced with permission^[20]. Copyright 2020, American Association for the Advancement of Science; (B) Suspension shear dip-coating method. Reproduced with permission^[95]. Copyright 2023, Springer Nature; (C) Electrochemical plating method. Reproduced with permission^[96]. Copyright 2023, John Wiley and Sons; (D) *In-situ* chemical reduction synthesis method. Reproduced with permission^[41]. Copyright 2022, Sage Publications; (E) Solution-redox method. Reproduced with permission^[97]. Copyright 2021, Royal Society of Chemistry; (F) Combination of direct dip-coating and electroplating processes. Reproduced with permission^[98]. Copyright 2021, American Chemical Society.

Physical coating and chemical plating processes can also be combined. For example, Han *et al.* developed a multifunctional coaxial energy fiber with a multilayer structure, using a combination of direct dip-coating and electroplating to create different functional layers on the fiber surface^[98] [Figure 5F]. By integrating various film-forming techniques, it is possible to form uniform and dense multilayer functional structures on micro-cylindrical surfaces, suitable for applications in sensing, actuation, and other scenarios. Physical coating and chemical plating technologies each have their advantages but face challenges in achieving high precision and consistency. Physical coating is limited by coating speed and substrate shape, while chemical plating is affected by reaction kinetics and deposition conditions. Optimizing process parameters and developing novel materials is crucial for enhancing the performance of micro-cylindrical electronics

fabrication.

Equivalent technologies for efficient production

Transfer printing^[21,35,45,99,100] and nanoimprinting^[101,102] techniques are advanced equivalent fabrication methods that focus on the precise replication and transfer of functional structures or flexible electronics onto high-curvature micro-cylindrical surfaces. Both techniques offer scalable, high-fidelity reproduction of intricate structures and are essential for integrating multifunctional electronic devices on curved substrates, overcoming the limitations of traditional planar manufacturing processes. They enable the creation of sensors, actuators, and other functional devices, providing a pathway for the mass efficient production of high-performance electronics on non-planar surfaces.

Transferring flexible electronics from planar onto curved surfaces

Transfer from planar to high-curvature micro-cylindrical surfaces is based on preparing planar thin-film devices using microelectromechanical systems (MEMS) processes for flexible electronics, which are then wrapped onto the micro-cylindrical surfaces using molds, adhesives, and other means^[21,35,45,99,100,103]. Lee *et al.* used a conventional method to prepare planar flexible thin-film electronics, relying on the good ductility of the substrate^[44], nested with an implantable micro-cylindrical device of about 1 mm in diameter to achieve fit by conformal bending [Figure 6A]. Liu *et al.* first fabricated a 1024-channel Neuroscroll probe electronic structure using planar MEMS processes and then wrapped it around a micro-cylindrical surface using a micro-tungsten wire as a carrier^[32], achieving a theoretical diameter of the micro-cylindrical structure of 84 and 138 μm [Figure 6B]. Pothof *et al.* transferred a 64-channel circuit structure onto a SEEG probe with an 800 μm diameter using a specialized rolling mold, and employed a Cytop adhesive layer to enhance the conformal attachment of the flexible circuit^[104]. Fiath *et al.* also used the same process to fabricate probe electrodes^[49], but innovatively designed the transfer mold to reduce processing errors when wrapping flexible circuits onto micro-cylindrical surfaces [Figure 6C]. Schwaerzle *et al.* designed an optical stimulation electrode by covering a micro-cylindrical substrate with flexible circuits^[105], with mechanical assembly and adhesive connections between thin-walled multilayer structures [Figure 6D]. The above studies designed different processing molds to achieve conformal transfer to micro-cylindrical substrates, aiming to minimize wrapping attachment errors and enhance structural adhesion. Overall, transfer techniques demonstrate remarkable replication capabilities and offer an effective means for integrating multifunctional electronic devices onto micro-cylindrical substrates. However, future efforts should prioritize enhancing transfer accuracy and device consistency on high curvature surfaces to further advance this technology.

Nanoimprinting for rapid 3D fabrication

The nanoimprinting process can replicate micro-nanostructures from molds onto high-curvature micro-cylindrical surfaces, with imprint quality depending on the mold design and imprinting method^[101,102]. Mekarū *et al.* designed a sliding planar mold technique suitable for polyester fibers with a diameter of 180 μm by utilizing rolling and sliding movements^[106] [Figure 7A]. This technique addresses the fiber twisting issue by clamping the fiber between heated metal cylinders and dynamically rotating the setup to match the fiber's rotation. During the process, the fiber rolls between two planar molds while being thermally imprinted with a 50 μm deep diffraction grating pattern, achieving a manufacturing precision of 50 μm .

The cylindrical mold technique includes two innovative approaches. Wang *et al.* used the draw-induced thermal drawing (DITD) method, in which a pair of rollers with the desired surface structures serve as a template^[38] [Figure 7B]. In this process, the softened material is stretched into fibers at a high drawing speed

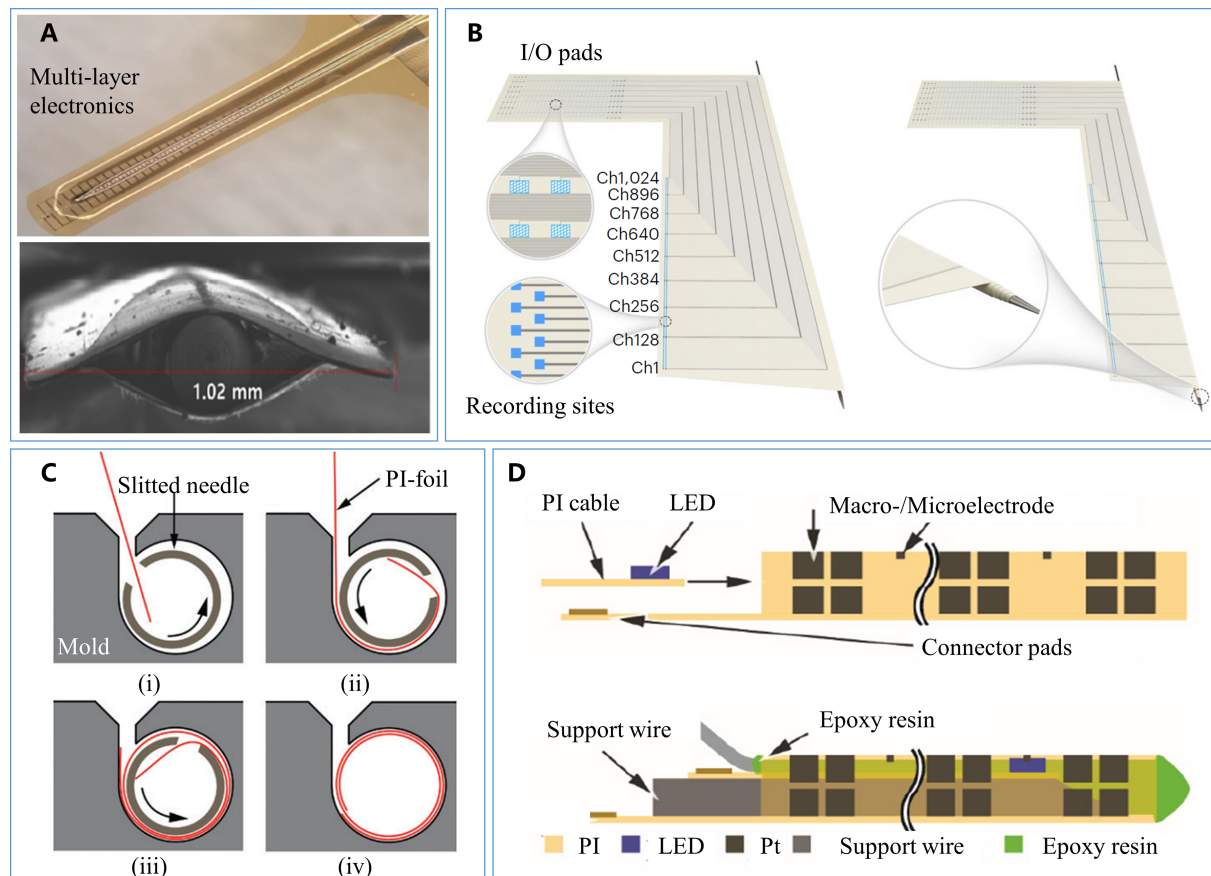


Figure 6. Transfer fabrication technology for micro-cylindrical electronics manufacturing. (A) Conformal bending of flexible thin film electronics. Reproduced with permission^[44]. Copyright 2024, Springer Nature; (B) Direct wrapping of flexible circuits on high-curvature micro-cylindrical surfaces. Reproduced with permission^[32]. Copyright 2024, Springer Nature; (C) Innovative wrapping mold design to reduce errors. Reproduced with permission^[49]. Copyright 2018, De Gruyter, Berlin/Boston; (D) Mechanical assembly and adhesive connection scheme for thin-walled multilayer structures. Reproduced with permission^[105]. Copyright 2015, Elsevier.

above the thermoplastic transition temperature, while the rollers imprint the fiber, achieving precise surface patterning. Ohtomo *et al.* employed a different method, using a cylindrical mold with hybrid layered microstructures to perform high-speed rolling on 240 μm diameter polymethylmethacrylate (PMMA) plastic optical fibers, achieving continuous surface patterning^[107] [Figure 7C]. These techniques achieve nanoscale manufacturing precision and are suitable for the functional design requirements of micro-diameter optical fibers. However, they still encounter challenges related to mold design and material adaptability. With ongoing optimization of the nanoimprinting process, these technologies are anticipated to play a significant role in the advancement of optical fibers, sensors, and other functional devices in the future.

APPLICATION

Fibric/micro-cylindrical electronic devices, as highly integrated miniature sensing and detection systems, have made remarkable strides in various fields in recent years, particularly in healthcare, life sciences, and environmental monitoring. These devices offer a wide range of application prospects due to their miniaturization, flexibility, implantability, and high sensitivity. In the healthcare sector, applications of micro-cylindrical devices can be categorized into two main areas: *in vitro* wearable monitoring and *in vivo* implantable monitoring. Wearable sensors facilitate personalized health management by continuously

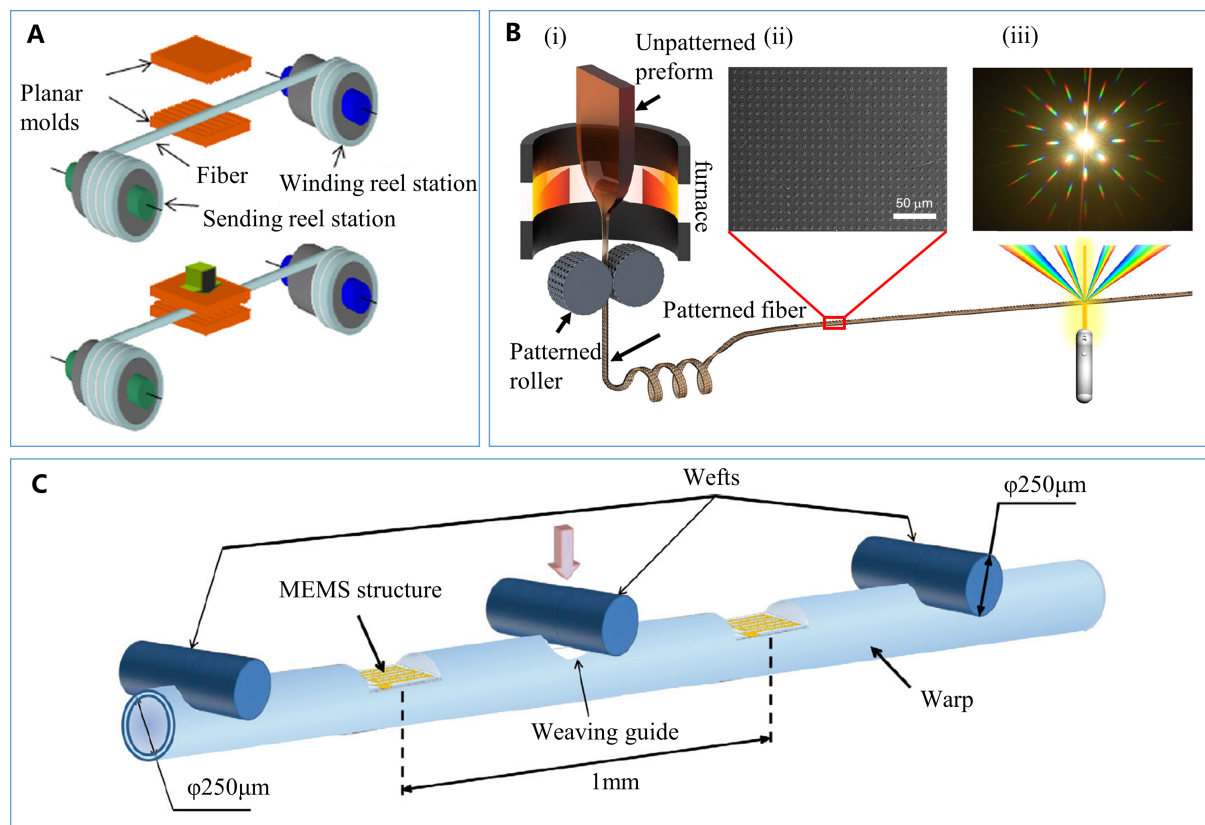


Figure 7. Nanoimprint fabrication technology on micro-cylindrical surfaces. (A) Nanoimprinting based on sliding planar molds. Reproduced with permission^[106]. Copyright 2011, American Vacuum Society; (B) High-temperature-assisted thermal drawing imprinting technique. Reproduced with permission^[38]. Copyright 2020, Springer Nature; (C) High-speed rolling based on cylindrical molds with hybrid layered microstructures. Reproduced with permission^[107]. Copyright 2013, Elsevier.

monitoring physiological data such as heart rate and blood pressure, while implantable biosensors provide accurate data essential for the early diagnosis and treatment of diseases by detecting biomarkers or physiological signals within the body. Additionally, high-sensitivity optical fiber sensors are mainly employed in environmental monitoring. These devices enable real-time monitoring of environmental parameters, including ambient temperature, gas concentration, and humidity. Additionally, micro-cylindrical electronics have demonstrated significant potential in surgical assistance. Surgical robots equipped with micro-cylindrical sensors enhance the precision and safety of minimally invasive procedures. Moreover, MRI marking technology offers effective support for real-time imaging and localization during surgery, allowing surgeons to operate with greater accuracy. Overall, micro-cylindrical electronics are transforming traditional practices in medical and environmental monitoring, driving these fields toward increased intelligence and precision.

Building upon advancements in applications across these fields, different areas impose varying requirements on the performance characteristics of fabric/micro-cylindrical electronic devices. To ensure seamless integration and optimal functionality across each domain, these devices must be specifically engineered to meet the unique demands of their respective sectors, as illustrated in [Table 5](#).

Wearable fabric electronics

Wearable sensors facilitate continuous, real-time, and non-invasive monitoring of environmental and physiological parameters, with broad applications in healthcare, sports health monitoring, electronic skin

Table 5. Requirements for micro-cylindrical/fibric electronics in different applications

| Application | Mechanical toughness | Biocompatibility | Environmental adaptation | Monitoring function | Ref. |
|---|------------------------------|---------------------------------|---|---|------------|
| Wearable fibric electronics | Flexible; stretchable | High biocompatibility | Temperature/humidity change resistance; vibration stability; mechanical deformations | ECG; temperature; humidity; pressure; strain | [108, 109] |
| Environmental monitoring | Rigid; flexible; stretchable | Medium biocompatibility | High/low temperature resistance; temperature/hu-midity change resistance; chemical corrosion resistance | Temperature; humidity; pressure; gas concentration; pH | [110, 111] |
| Micro-cylindrical sensors for surgical robots | Rigid | High biocompatibility | Temperature change resistance; vibration stability | Temperature; pressure; strain | [112-114] |
| Implantable probe bioelectronics | Flexible | Extremely high biocompatibility | Chemical corrosion resistance; vibration stability | SEEG; temperature; strain; glucose; neurotransmitter; oxygen partial pressure; cation composition; pH | [34, 115] |
| Interventional MRI resonant markers | Flexible | High biocompatibility | Strong magnetic field adaptability; temperature change resistance | 3D imaging | [116, 117] |

ECG: Electrocardiogram; SEEG: stereo electroencephalogram; MRI: magnetic resonance imaging.

(e-skin), and human-computer interaction^[108,118]. Desirable wearable sensors must exhibit excellent flexibility and stretchability to accommodate the complex body structures and mechanical deformations encountered during daily activities^[119,120]. Conventional thin-film-based flexible e-skins predominantly utilize planar or thin-film structures, and numerous studies have advanced their flexibility, conformity, and multifunctionality^[121-123]. For example, e-skins fabricated from ultrathin materials adhere closely to the skin, enabling precise acquisition of biomechanical and bioelectrical signals^[124]. Additionally, research has developed stretchable e-skins capable of capturing multiple physiological signals in dynamic conditions^[125-127]. Thin-film wearable sensors excel in signal acquisition accuracy, multimodal sensing, and material ductility^[128,129]. In contrast, fibers, characterized by their robustness, ease of handling, and deformability, offer an ideal platform for integrating sensor devices^[109,130]. Furthermore, fiber sensors can be woven into flexible, deformable, and breathable textiles, further broadening their application scope. This section will focus on wearable fibric mechanical sensors, as well as wearable fibric thermal sensors, exploring their sensing principles, common structures, and typical applications in accordance with current demand scenarios and major research trends.

Fibric mechanical sensors

Fibric strain sensors are capable of swiftly detecting physical responses and converting mechanical deformations into electrical signals. These sensors exhibit fast response times, broad sensing ranges, excellent compliance, and can be seamlessly integrated into textiles, making them highly suitable for applications in human health monitoring and motion state detection. Fiber-based strain sensors can be categorized by their sensing mechanisms into resistive^[131], capacitive^[132], piezoelectric^[133], triboelectric^[134], and optical types^[135].

Resistive fibric strain sensors measure the magnitude of strain by detecting changes in resistance under mechanical stretching. These sensors are widely used due to their simple structure and ease of fabrication^[58,108]. Huang *et al.* developed a highly flexible and sensitive strain sensor based on a composite yarn^[41] for real-time effective recognition of sign languages. The performance of fiber sensors can be enhanced through material processing and unique microstructural designs^[136]. For example, optimizing the volume fraction of conductive nanofillers can improve sensitivity, while employing structural methods, such as wrinkled or helical configurations, can expand the strain sensing range^[120,137]. However, the viscoelastic

behavior of polymer materials can lead to poor hysteresis properties in resistive fibric strain sensors, a challenge that must be addressed to enhance their stability and reliability.

Triboelectric fiber-based strain sensors operate on the principle of converting external deformations caused by the frictional interaction between two fiber-based materials with differing electron affinities into electrical signals^[138,139]. These sensors are widely employed in healthcare applications due to their simple structure, high accuracy, and unique self-powered characteristics^[140]. A typical triboelectric fiber-based strain sensor is designed with a helical structure^[141]. Upon stretching, the contact state between the two triboelectric layers changes, generating an electrical signal. Consequently, helical fiber strain sensors (HFSSs) are utilized to monitor human respiration [Figure 8A and B]. Additionally, triboelectric fiber-based strain sensors can be configured in a single-electrode mode [Figure 8C]. Conductive yarn is fabricated by twisting several polyester microfibers together with a stainless-steel microfiber, resulting in excellent sensitivity^[142]. This sensor can be easily integrated into gloves for gesture recognition [Figure 8D]. It is important to note that triboelectric fiber-based strain sensors often develop surface defects due to repeated friction during prolonged operation, which can negatively affect sensing performance. These surface defects can be mitigated or prevented through the application of advanced surface treatment technologies.

Capacitive fiber-based strain sensors respond to strain by altering their capacitance. These sensors typically employ a core-shell structure^[143], which is effective for detecting elongation strain. These sensors can be integrated into textiles through sewing or weaving, enabling real-time monitoring of wearer movement during activities such as walking [Figure 8E and F]. Beyond the core-shell design, capacitive fiber-based strain sensors often utilize a double helical structure^[29]. For instance, Lee *et al.* reported a fiber strain-sensing system based on a helical structure consisting of two conductive fibers^[144], which offers stability, durability, and excellent sensitivity. Furthermore, the response of capacitive fiber-shaped strain sensors is particularly sensitive to changes in the dielectric constant of the surrounding environment. To address this limitation, it is essential to develop analytical models that account for various environmental conditions.

In addition to fibric strain sensors, fibric pressure sensors are also extensively utilized in motion monitoring, human-computer interaction, and e-skin due to their simple structure, low power consumption, and skin compatibility^[145]. Similar to fibric strain sensors, fibric pressure sensors can be categorized based on their sensing mechanisms into resistive, capacitive, electromagnetic, triboelectric, and optical pressure sensors.

Resistive fibric pressure sensors detect pressure by altering conductive paths under applied pressure, leading to a change in resistance. To date, various conductive materials, including CNTs, graphene, MXene, and metals, have been employed in the fabrication of fibric pressure sensors. Lan *et al.* developed conductive Au-MoS₂ composite-coated fibers exhibiting superior electrical conductivity, tensile strength, and stability^[146]. By stacking two Au-MoS₂ composite-coated fibers perpendicularly, a pressure sensor is formed at their cross-contact point [Figure 8G]. Integration of the pressure sensor into a fabric glove allows for multiple force mapping properties [Figure 8H and I]. The sensitivity of wearable sensors can be significantly enhanced through the use of advanced fiber materials and innovative microstructural designs. For example, fibric pressure sensors with high compressibility and sensitivity have been developed using hierarchical three-dimensional, porous reduced graphene oxide (rGO) fibers as key sensing elements^[147]. These sensors can effectively monitor human respiration and pulse [Figure 8J and K]. Additionally, highly sensitive fibric pressure sensors have been fabricated by fabricating stretchable MXene/CNT/polyurethane (PU) fibers via a wet spinning technique^[148].

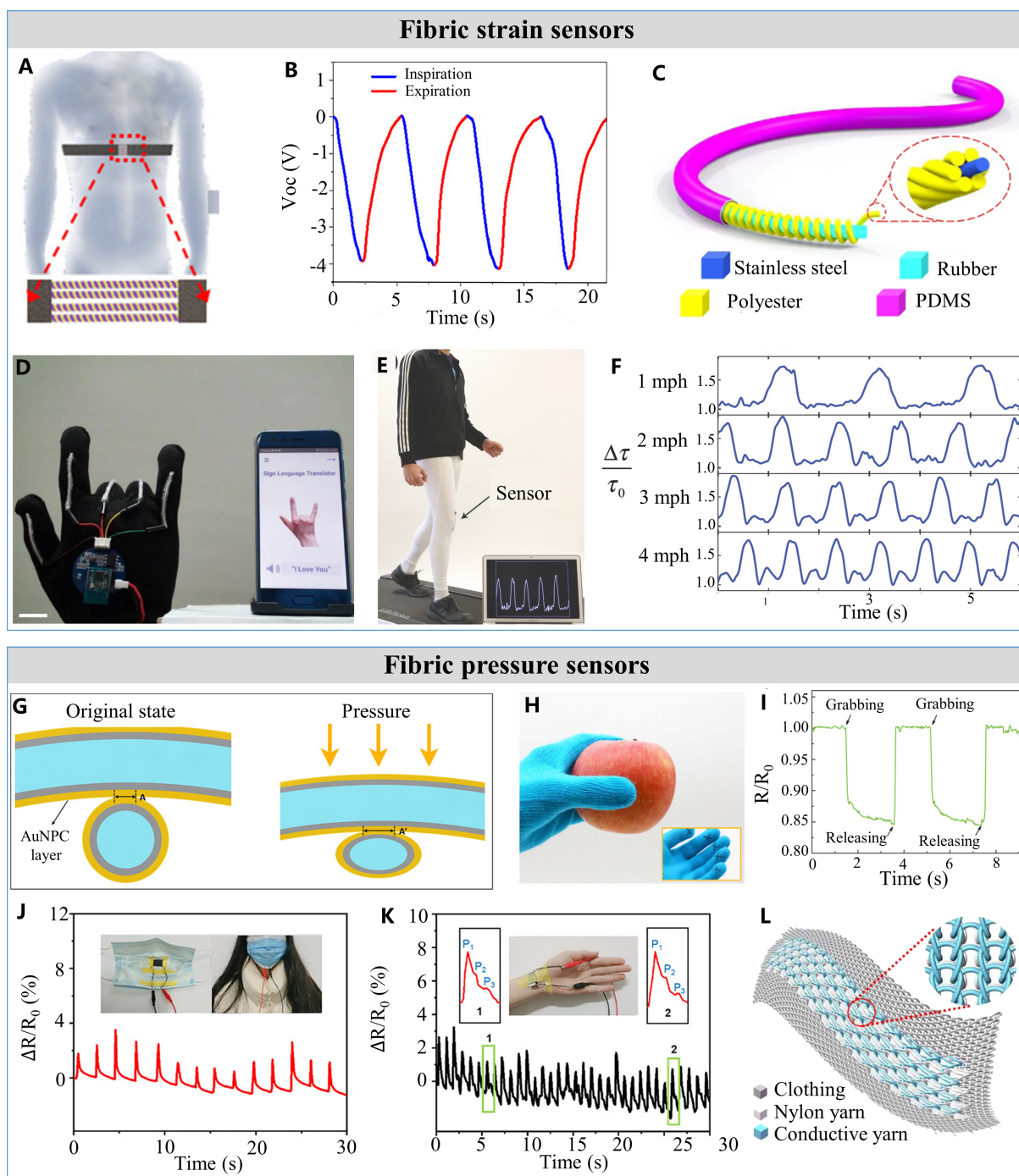


Figure 8. Principle, structure and application of fibric strain and pressure sensors. (A) Schematic diagram of a chest strap integrated with HFSSs; (B) Routine electrical signals from the HFSS-based chest strap during human respiration^[141]. Copyright 2022, American Chemical Society; (C) Illustration of the yarn-based stretchable sensing device; (D) Photographs of the wearable sign-to-speech interpretation system^[142]. Copyright 2020, Springer Nature; (E) Capacitive soft strain sensor mounted on textile across the knee; (F) Normalized decay time of the sensor output at different walking speeds^[143]. Copyright 2015, John Wiley and Sons; (G) Schematic illustration showing structural change of the pressure sensor under the applied pressure; (H) Photograph of a human hand wearing the smart glove with five pressure sensors on each finger when grabbing an apple; (I) Resistance response of the pressure sensor when grabbing and releasing an apple^[146]. Copyright 2020, American Chemical Society. Application of wearable devices for (J) detecting breathing and (K) monitoring pulses^[147]. Copyright 2019, American Chemical Society; (L) Schematic diagram of a fibric triboelectric sensor in combination with clothing. Reproduced with permission^[151]. Copyright 2020, American Association for the Advancement of Science. HFSSs: Helical fiber strain sensors.

Capacitive fibric pressure sensors are known for their high accuracy, wide detection range, and reliability. For effective performance, the fiber electrodes must maintain stable conductivity during stretching and bending^[149]. Additionally, microstructures can be incorporated to enhance sensing capabilities and reduce response time^[150]. Furthermore, one-dimensional conductive fibers, such as gel fibers, CNT fibers, graphene fibers, and polyaniline fibers, can be used as electrodes for capacitive pressure sensors, forming fiber electrode pairs. For example, fiber pressure sensors made with hydrogel exhibit high sensitivity, a wide operating range, and stable proximity sensing^[65].

When piezoelectric materials such as ZnO, BaTiO₃, and polyvinylidene fluoride (PVDF) are subjected to pressure, deformation of their crystal structure occurs, resulting in charge separation and the generation of voltage across the material. These piezoelectric materials are widely used in the development of piezoelectric fiber-based pressure sensors. For instance, integrating a fibric triboelectric sensor array into clothing enables simultaneous monitoring of arterial pulse and respiratory signals^[151], facilitating non-invasive and long-term health surveillance [Figure 8L]. Additionally, a piezoelectric PVDF nanofiber membrane (PVDF/ZnO NFM) was utilized as the pressure sensing layer^[152]. This textile was used for external pressure detection, human pulse monitoring, and tactile spatial mapping. Despite the high durability and flexibility of piezoelectric fibric pressure sensors, they are generally limited to dynamic measurements. However, by integrating a rectifier component, continuous measurements can be achieved.

Fibric thermal sensors

Body temperature monitoring is essential for assessing health conditions. However, traditional temperature sensors are unsuitable for wearable applications due to their rigidity and inability to provide continuous body temperature monitoring over extended periods^[153,154]. Fibric temperature sensors, by contrast, offer high sensitivity, rapid response, along with the flexibility and compliance to the skin^[5], making them widely applicable in e-skin^[155] and healthcare^[156]. Based on the temperature sensing mechanisms of the temperature-sensitive materials, fibric temperature sensors can be categorized into thermoresistive and thermoelectric types. The functional materials, structural designs, performance, and application areas of these two types of fibric temperature sensors will be discussed in detail in the following sections.

The principle of thermoresistive fibric temperature sensors is that resistance changes with temperature^[157]. The conductive polymer poly(3,4-ethylenedioxythiophene)-poly(styrenesulfonate) (PEDOT:PSS) shows strong potential for wearable temperature sensing due to its excellent flexibility, good electrical conductivity and high sensitivity^[153,158]. Furthermore, to mitigate the impact of additional stress, various specialized structural designs have been employed in the development of strain-insensitive fibric temperature sensors. One option is that a strain-insensitive fibric temperature sensor with periodic and uniform micro-wrinkles can be fabricated by applying pre-strain^[159]. Another feasible option is to sew PEDOT-thermoplastic polyurethane (TPU) composite fibers into normal textiles in an S-shape, which allows the sensor to measure skin temperature accurately during daily activities^[160] [Figure 9A]. However, as a polymer, PEDOT fibers are vulnerable to humidity, leading to inaccurate measurements, especially after perspiration. To address this issue, temperature-sensitive fibers have been developed by encapsulating PEDOT with a PU/graphene composite^[153] [Figure 9B]. Carbon-based materials are also widely employed in fibric temperature sensors due to their high electrical conductivity and thermal stability, such as graphene oxide (GO)-based fibers^[161], rGO/PU composite freestanding stretchable fibers^[162], and graphene-based fibers^[163]. Additionally, temperature-sensitive fabrics made from textile yarns coated with graphene-based inks offer both good washability and high flexibility^[163] [Figure 9C]. Fibric temperature sensors based on conductive polymers achieve high sensitivity, owing to their tunable semiconductor properties^[164,165]. When these sensors were integrated into textiles, they offered stable performance in detecting both body temperature changes and

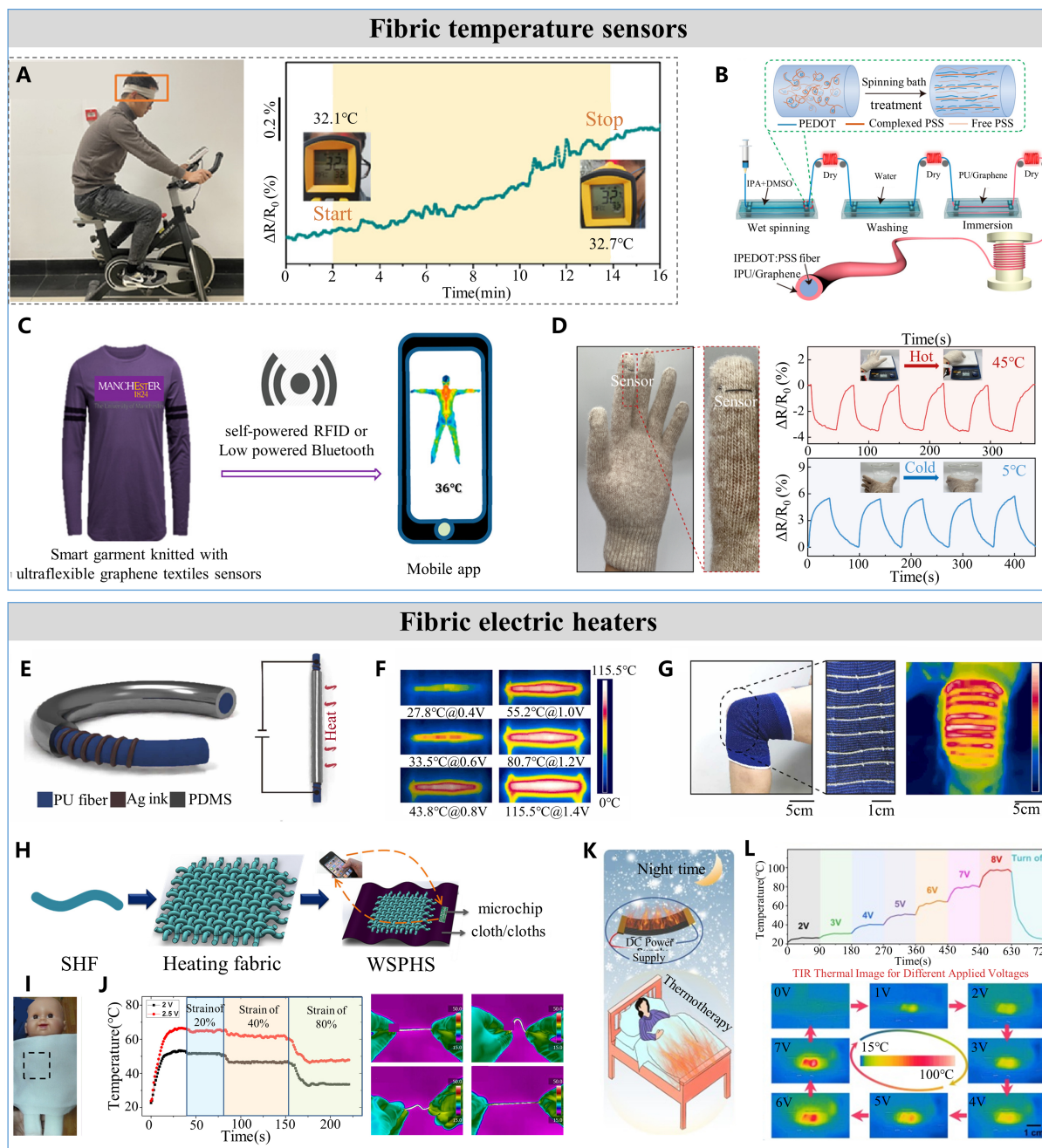


Figure 9. Principle and structure and application of fibric temperature sensors and heaters. (A) Tester wearing a headband with sensors and sensor response during cycling^[160]. Copyright 2022, American Chemical Society; (B) Preparation of PU/graphene encapsulated PEDOT:PSS composite fiber with skin-core structure^[153]. Copyright 2023, American Chemical Society; (C) Garment knitted with ultraflexible graphene textile sensors used for monitoring human physiological conditions^[163]. Copyright 2019, American Chemical Society; (D) Image of the fiber temperature sensor sewn onto the tip of a hand glove and temperature response of the fiber sensor to repetitive touch on a hot (45 °C) or cold (5 °C) object^[165]. Copyright 2023, Springer Nature; (E) Diagram of 1D SEF for wearable electrothermal applications; (F) Infrared thermal images of 1D-SEF at different applied voltages; (G) Optical and infrared thermal images of 1D-SEF embedded in a wearable kneepad with an applied voltage of 0.8 V^[15]. Copyright 2023, Elsevier; (H) Schematic of the integration process of WSPHS; (I) Photograph of WSPHS application at the chest position of an infant model; (J) Heating performance of stretchable heating fiber under various mechanical deformations^[170]. Copyright 2016, American Chemical Society; (K) DCFBs for all-weather personal thermal management textiles; (L) Temperature evolution and infrared thermal images of the fabric woven by DCFBs under stepwise voltage from 2 to 8 V^[171]. Copyright 2024, Elsevier. PU: Polyurethane; PEDOT:PSS: poly(3,4-ethylenedioxythiophene)-poly(styrenesulfonate); SEF: fiber-shaped electronics; WSPHS: wearable and smart personal heating system; DCFBs: dopamine-induced composite fiber bundles.

touch-induced temperature variations [Figure 9D].

Thermoelectric fibric temperature sensors utilize the thermoelectric effect between two different conductors to measure temperature. When one end of the thermocouple is exposed to a temperature gradient, the potential difference between the conductors varies with the temperature^[108]. Wang *et al.* employed electrospinning technology to fabricate an elastic poly(styrene-block-butadiene-block-styrene) (SBS) nanofiber mat, which was subsequently drop-coated with a PEDOT:PSS solution to form a uniform shell layer. This process resulted in a temperature-sensitive layer with advantages including linearity, high sensitivity, and stability^[166].

Wearable electric heaters have broad applications across various fields, including healthcare^[167] and personal thermal management^[168]. Fibric electric heaters allows for more efficient integration of conductive materials, as well as their inherent flexibility^[169]. Moreover, they can be woven into a variety of flexible and breathable fabrics^[23]. Fibric electric heaters can be achieved by printing metallic materials directly onto the surface of elastic fibers to create. For instance, helical silver electrodes can be printed onto the surface of PU fibers and encapsulated with polydimethylsiloxane (PDMS)^[15] [Figure 9E and F]. The helical structure provides the fibers with excellent stability, softness, and stretchability, allowing them to be woven into items such as kneepads and gloves [Figure 9G]. Additionally, coating fibers or textiles with a layer of metal or metal oxide nanowires represents another viable approach for the development of fibric electric heaters. For instance, Cheng *et al.* designed a copper nanowire (CuNW) composite fiber with a unique hierarchical structure^[170] [Figure 9H]. This fiber not only exhibits excellent heating performance but also demonstrates remarkable tolerance to mechanical impacts, such as bending, twisting, and stretching. It has been applied as a heating layer for infant warming coats [Figure 9I and J]. Currently, the preparation of stretchable conductive fibers is complex and these fibers are prone to failure under significant deformation, which limits their application. To address this issue, Li *et al.* enhanced the wettability of PU multi-filaments using dopamine. They then coated the filaments with striated polypyrrole (PPy), resulting in composite fiber bundles with excellent stability and strain-insensitive properties. These composite fibers were integrated into smart textiles and demonstrated considerable potential for use in wearable thermal therapy devices^[171] [Figure 9K and L].

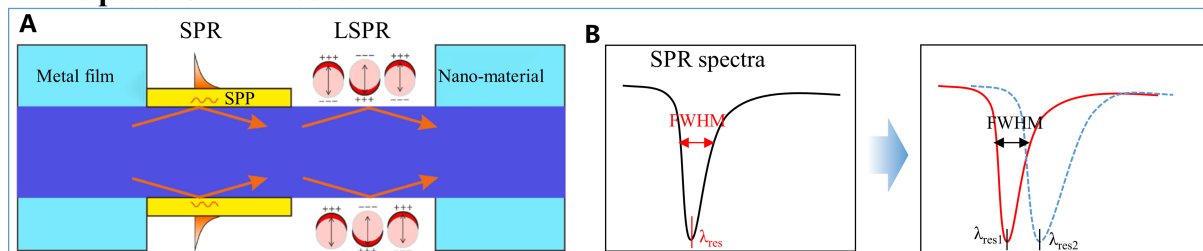
Optical fiber sensors for environmental monitoring

SPR-based optical fiber sensors

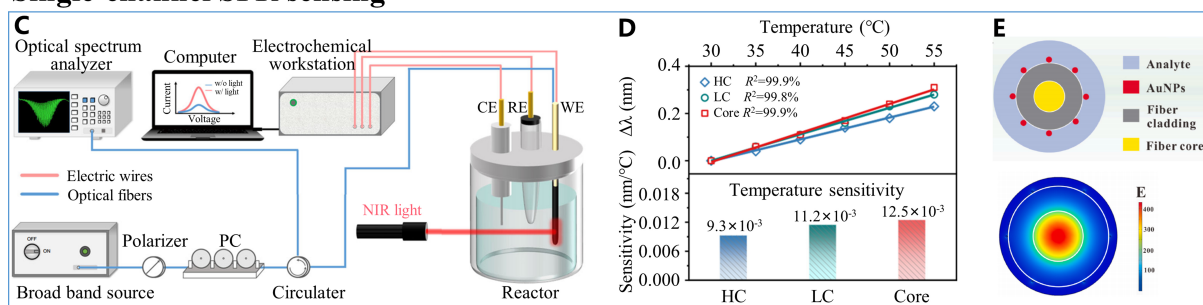
Optical fibers, as a typical fibric device, offer significant advantages in long-distance monitoring, miniaturization, and the flexible manipulation of light. Sensing based on the surface plasmon resonance (SPR) effect can be achieved by fabricating functional coatings on the surface of optical fibers^[110]. When the incident light and surface plasmon polaritons (SPP) satisfy the wavevector matching condition, a portion or most of the incident light energy couples into the SPP [Figure 10A]. When the refractive index of the surrounding environment changes, characteristics such as the SPR wavelength and the half-peak width detected by the spectrometer will also change in response [Figure 10B]. Nanomaterials such as AuNPs^[172], CNTs^[173], silicon oxide (SiO₂)^[174], and GO^[175] are commonly used in these coatings. Due to the extreme sensitivity of SPR effect to the refractive index of the surrounding environment, it is frequently utilized in biological and chemical detection applications.

In general, the performance of fiber optic SPR sensors is heavily influenced by the material and thickness of the metal film. Gold is widely utilized for SPR sensing owing to its stable chemical properties and high dielectric constant^[176]. Li *et al.* proposed a sensing system based on gold-plated single-mode optical fibers with a tilted fiber Bragg grating (TFBG) etched in the fiber core^[177], as shown in Figure 10C. The spectral

Principle of SPR sensors



Single-channel SPR sensing



Multi-channel SPR sensing

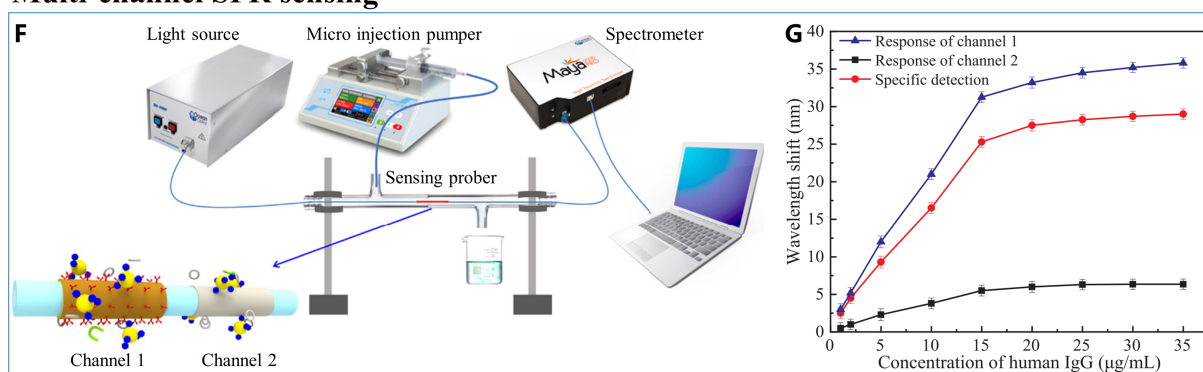


Figure 10. Principle and application of fiber optic SPR sensors. (A) Principle diagram of the optical fiber sensor based on SPR and LSPR. Reproduced with permission^[110]. Copyright 2024, Elsevier; (B) Changes in the SPR spectra during the sensing process; (C) SPR optical fiber temperature sensing system for *in situ* monitoring of thermal effects in photoinduced catalysis; (D) Thermal sensitivity of HC mode, LC mode, and fiber core mode to varying ambient temperatures. Reproduced with permission^[177]. Copyright 2022, Springer Nature; (E) Cross-sectional of the fiber optic LSPR sensor based on AuNPs coating, along with a fundamental mode analysis of the sensor. Reproduced with permission^[179]. Copyright 2023, Elsevier; (F) Composition of a dual-channel SPR detection system designed for synchronized human IgG sensing and temperature compensation; (G) Wavelength shift of the dual-channel SPR sensor at varying human IgG concentrations. Reproduced with permission^[190]. Copyright 2019, Elsevier. SPR: Surface plasmon resonance; LSPR: localized surface plasmon resonance; HC: high-order cladding; LC: low-order cladding; AuNPs: gold nanoparticles; IgG: immunoglobulin G.

transmission of these devices can differentiate between rapid changes in localized temperature at the catalyst surface and rapid changes in ambient temperature. Thermal effects in interfacial photoinduced catalysis can be decoded with a temperature resolution of 0.1 °C and a time resolution of 0.1 s [Figure 10D]. Recently, Villatoro *et al.* employed the deposition of a gold film on one side of a TFBG to create a dual-resonance structure^[172]. It achieves high sensitivity in refractive index detection while also compensating for temperature fluctuations.

In addition to metal materials, a variety of new nanomaterials have been widely used, operating on a slightly different principle from SPR. This principle involves constructing localized surface plasmon resonance (LSPR) on the surface of nanoparticles^[178]. Ning *et al.* introduced a bent-structure J-shaped fiber optic

probe, forming the basis of a LSPR biosensor for the detection of *Helicobacter pylori* (*H. pylori*)^[179]. This biosensor was achieved by coating the fiber surface with AuNPs and specific aptamers, as shown in [Figure 10E](#). CNTs have been selected as sensing materials for fiber optic LSPR sensors due to their unique advantages, including high chemical stability and large surface area. An example is a fiber optic SPR sensor based on multi-walled CNTs (MWCNTs)-PPy matrix for dopamine detection^[180]. In addition, nanoparticles such as SiO₂^[181,182], ZnO^[183,184], TiO₂^[185-187], and MoS₂^[188] have been used in LSPR-based fiber-optic sensors for detecting gas concentration, humidity, specific ion concentration, and other parameters. LSPR generates a locally enhanced electromagnetic field, which makes LSPR particularly suitable for detecting localized environmental changes or specific markers.

To further improve the detection accuracy and expand the application range of fiber optic SPR sensors, multi-channel SPR sensors have been developed. These sensors compensate for non-specific binding and allow for the simultaneous determination of multiple analytes^[176,189]. Wang *et al.* proposed a dual-channel self-compensating fiber optic SPR sensor for the detection of human immunoglobulin G (IgG)^[190]. One sensing channel was coated with a bilayer of GO and gold to detect human IgG labeled with AuNPs. The other sensing channel was coated with a silver film only, serving as a reference channel [[Figure 10F](#)]. The sensor's detection limit for human IgG was reduced to 15 ng/mL, which is superior to the detection limit of conventional SPR sensors [[Figure 10G](#)]. Siyu *et al.* designed a dual-channel SPR sensor based on a hollow-core fiber (HCF)^[191]. Coating the inner and outer surfaces of the HCF with silver and gold films, respectively, enables the simultaneous measurement of seawater salinity and temperature. Recently, Zheng *et al.* deposited AuNPs/ β -cyclodextrin (β -CD) composites onto a gold-film-coated HCF and filled the inner channel with glycerol as a temperature-sensitive material^[192]. This setup effectively induced both the SPR effect and the multi-mode interference (MMI) effect, enabling simultaneous measurement of cholesterol concentration and temperature.

The application of optical fiber sensors in environmental monitoring has highlighted their significant advantages in high-sensitivity detection, particularly through SPR and LSPR technologies. However, current techniques face challenges, such as crosstalk among multiple physical signals and distributed sensing. Looking ahead, the ongoing development of new materials and advancements in multi-channel sensing technology are expected to expand the applications of optical fiber sensors in areas such as bio-detection and gas concentration monitoring, thereby facilitating the evolution of intelligent environmental monitoring systems.

POF sensor with surface functionalization

Traditional silicon-based optical fibers have been developed over several decades and are renowned for their high light conduction efficiency. However, their inherent brittleness constrains the range of potential application scenarios. In contrast, POFs, made from polymers with superior bending flexibility, can withstand larger strains, making them ideally suited for flexible sensors. Functional microstructures processed on the POF surface enable single or multi-mode sensing^[54,193], including strain^[194,195], temperature^[111], heart rate^[196], blood monitoring^[30,197], *etc.* Specific approaches include increasing the surface area to enhance inter-fiber friction^[198], creating arrayed micro-nano structures for specialized optical applications^[199,200], and even integrating electronic devices directly onto the POF surface^[42,201].

Nanoimprinting technology is well-suited for fabricating arrayed micro- and nanostructures on the surface of POFs or other functional fibers, offering high throughput and high resolution. Mekaru *et al.* conducted an extensive study using this process, preparing dot-array structures on the surface of 250- μ m-diameter POFs with a length of 1.6 m using roller nanoimprinting technology^[202] [[Figure 11A and B](#)]. Additionally,

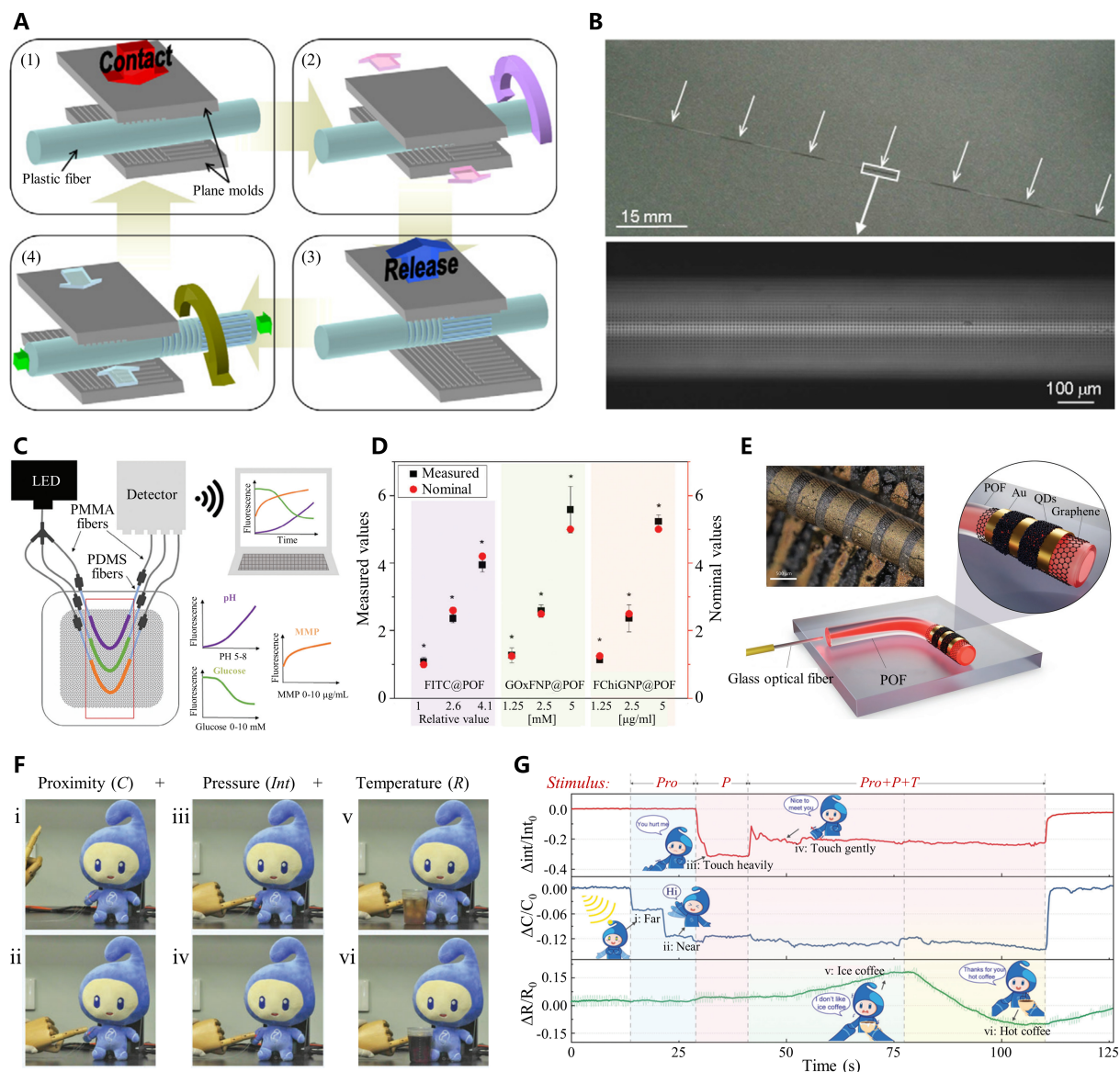


Figure 11. Application of plastic optical fibers with surface functional patterning. (A) Procedure of roller imprinting on the POF surface; (B) Photograph of intermittently patterned POF (top) and optical micrograph of 5 μm dotted pattern imprinted on POF (bottom). Reproduced with permission^[202]. Copyright 2010, Elsevier; (C) Setup scheme required for multi-sensing fluorescent POF sensors; (D) Multi-sensing device individually tested using nine complex solutions with different pH, glucose concentration, and MMP concentration. Reproduced with permission^[206]. Copyright 2023, John Wiley and Sons; (E) Schematic and optical image of a printed hybrid PbS QDs phototransistor structure. Reproduced with permission^[42]. Copyright 2023, John Wiley and Sons; (F) Photograph of multimodal human-computer interaction using an optoelectronic multimodal sensor; (G) Relative rates of change in intensity, capacitance, and resistance during the interaction with multiple stimuli existing simultaneously. Reproduced with permission^[201]. Copyright 2023, John Wiley and Sons. POF: Polymer optical fiber; MMP: matrix metalloproteinase; QDs: quantum dots.

smart fiber optic sensors with multiple sensing functions are expected to be realized through the structuring of arrays of diffraction gratings^[106,199,203] or MEMS structures^[200] on the POF surface. Nanoimprinting technology can achieve high-resolution manufacturing by combining with photolithography templates^[107], and the roll-to-roll process further improves production efficiency^[22,199,204,205]. However, it is necessary to ensure compatibility between the mold material and the fiber optic material during application to avoid compromising the basic function and structure of the optical fiber.

In addition to nanoimprinting, chemical coating is a common method for preparing functional structures on POF surfaces. Unlike SPR-based fiber optic sensing, functional structures coated on POFs can be utilized for a variety of fluorescence-based sensing applications^[54]. Recently, Giovannini *et al.* developed a multi-sensing platform using three fluorescein isothiocyanate (FITC)-based POF sensors for the efficient quantification of pH, glucose, and matrix metalloproteinase (MMP) concentrations present in the wound exudate^[206] [Figure 11C and D]. Moreover, inkjet printing technology is emerging as a promising method for preparing functional structures on POF surfaces and has been used to fabricate POF-based photodetector devices. For instance, Kara *et al.* printed colloidal PbS quantum dots (QDs) on a 1-mm-diameter POF surface wrapped with graphene, working as infrared phototransistors^[42] [Figure 11E]. The fabricated device detects photocurrents under laser excitation to monitor scattered light in a multi-mode POF without interrupting the optical path. In 2023, Wang *et al.* reported a flexible optoelectronic multimodal sensor capable of detecting and decoupling proximity, pressure, and temperature signals^[201] [Figure 11F and G]. This was achieved by integrating an interdigital electrode on the POF surface to detect capacitance, light intensity, and resistance signals, respectively. This multifunctional and integrated self-decoupled multimodal POF sensor presents promising opportunities for human-machine-environment interaction applications. In brief, surface modification-based POF sensors exhibit significant potential for diverse applications in environmental signal monitoring, particularly due to their flexibility and versatility. In the future, these sensors are anticipated to play an increasingly vital role in fields such as medical monitoring, environmental protection, and smart home technologies.

Micro-cylindrical sensors for surgical robots

Surgical robots enhance the precision of surgeons during minimally invasive procedures, addressing challenges such as low standardization and the high risks associated with manual operations. A robotic surgical system typically comprises two key components: the robotic arm and the end-effector. The robotic arm, with its multiple degrees of freedom, is primarily responsible for controlling the manipulation of surgical instruments^[207]. The end-effector, which may include tools such as medical needles, forceps, or suturing devices, performs the actual surgical tasks. Precise motion control remains a critical challenge in current robotic surgical systems, which can be addressed through feedback control by monitoring the surgical site^[24]. Medical needles, as typical micro-cylindrical surgical instruments, can be equipped with sensors at the tip to enable real-time monitoring of the surgical environment, ensuring smooth and accurate operation.

Medical needles are among the most essential and widely used tools in medical procedures. They are extensively applied in various fields, including blood collection, drug administration, biopsy, and tissue ablation^[208]. Traditionally, impedance measurements for accurate localization of the needle rely on the needle body as a conductor^[209], which can constrain electrode design and configuration. This limitation can be addressed by fabricating electrodes directly onto the needle surface^[46]. For example, Yun *et al.* used spray coating and photolithography with a film photomask to fabricate microelectrodes on the needle surface [Figure 12A and B]. These microelectrodes enable measurements of the electrical impedance of biological tissues and the penetration depth of the needle^[51] [Figure 12C]. Furthermore, the flexibility of electrode design can be further enhanced by fabricating microscale electrode arrays on a PI membrane and co-conformally wrapping them onto the needle surface^[2]. Such integrated biosensor needle systems have been employed for multiparameter measurements, providing real-time tissue identification^[113] and enabling early detection of extravasation during intravenous infusion therapy^[114].

Different tissues exhibit significant variations in mechanical properties such as stiffness, viscoelasticity, and acoustic impedance. By analyzing these mechanical characteristics, it is possible to both differentiate between tissues and accurately determine the needle's position^[210]. Tissue stiffness can be quantified using

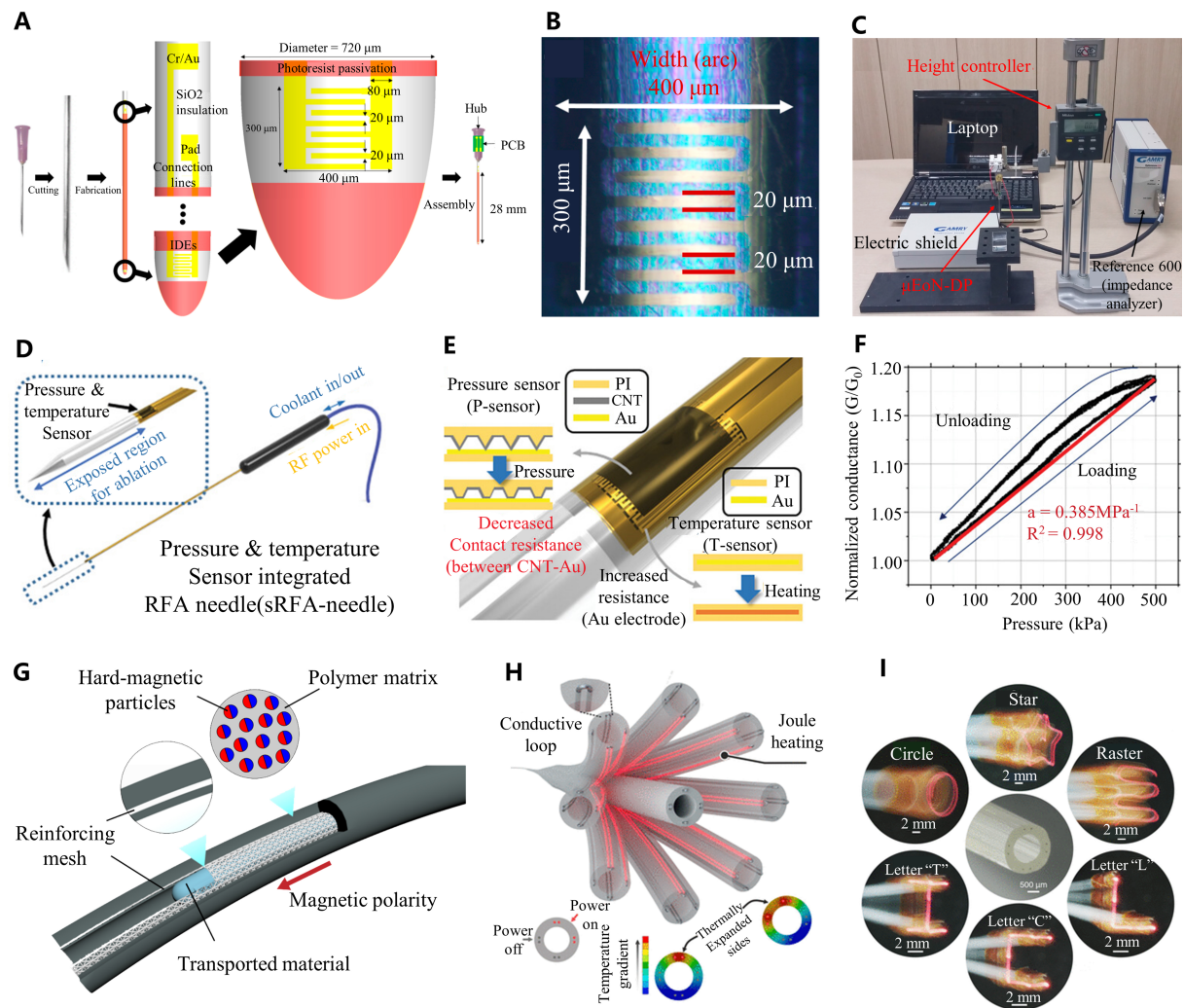


Figure 12. Principle application of micro-cylindrical sensors for surgical robots and microfiberbots. (A) Schematic design of the micro EIS-on-a-needle for depth profiling ($\mu\text{EoN-DP}$); (B) Photograph of the IDE fabricated on the curved surface of the needle; (C) Images of experimental setup. Reproduced with permission^[51]. Copyright 2016, MDPI; (D) Schematic of the overall system of the sRFA-needle; (E) Schematic of the operating principles of contact resistance-based P-sensor and resistance-based T-sensor; (F) P-sensor at hydrostatic pressure. Reproduced with permission^[211]. Copyright 2021, John Wiley and Sons; (G) A schematic representation of the FSCR, comprising a soft polymer matrix embedded with hard magnetic particles and reinforced with a PLA mesh. Reproduced with permission^[214]. Copyright 2021, Springer Nature; (H) Schematic of fiber cantilever bending driven by thermal expansion; (I) Six tip displacement patterns captured using the slow shutter speed function of a mirrorless camera while moving a $500\text{-}\mu\text{m}$ optical fiber connected to a 650-nm LED. Reproduced with permission^[112]. Copyright 2024, American Association for the Advancement of Science. EIS: Electrical impedance spectroscopy; IDE: interdigitated electrode; sRFA: sensor-integrated radiofrequency ablation; FSCR: ferromagnetic soft catheter robot; PLA: polylactide; LED: light-emitting diode.

acoustic impedance^[24], and medical needles with integrated acoustic impedance sensors are widely utilized for this purpose. Additionally, in radiofrequency (RF) ablation, heat-induced steam popping may occur, causing tissue necrosis. To mitigate this risk, Jeong *et al.* developed a flexible pressure sensor that operates based on the variation in contact resistance between an electrode and a three-dimensional microstructured PI/CNT composite film^[211,212] [Figure 12D and E]. By integrating both pressure and temperature sensors into the surface of an ablation needle, real-time monitoring of temperature and pressure is possible during procedures [Figure 12F]. During needle insertion, mechanical deformation occurs due to tissue reaction forces. This deformation can be assessed by integrating strain sensors, enabling more precise needle

positioning^[213].

The need for miniature and flexible robots for precise instrument guidance in minimally invasive surgeries is growing, and fiber robots present a viable solution. For instance, the ferromagnetic soft catheter robot (FSCR) system enables minimally invasive *in situ* bioprinting within living organisms^[214]. By incorporating ferromagnetic particles into a fiber-reinforced polymer matrix, the system successfully achieved *in vivo* hydrogel printing in a rat model [Figure 12G]. Similarly, Abdelaziz *et al.* developed a polymer-based robotic fiber using a fiber-drawing technique, with thermal actuation achieved through localized heating along the fiber's length. This fiber robot exhibits excellent motion accuracy and repeatability, making it a promising tool for delicate surgical procedures^[112] [Figure 12H and I]. Overall, both sensors at the tips of surgical instruments and fibric surgical robots have markedly enhanced the precision and safety of minimally invasive surgery. This advancement reduces the risks associated with traditional surgical methods by enabling real-time monitoring of the surgical environment and tool positioning.

Implantable probe bioelectronics

Implantable SEEG and DBS electrodes

Implantable neuroelectrodes refer to electrophysiological devices that are implanted within a biological organism and connected to it for the purposes of recording and stimulation^[215]. They are particularly valuable in the diagnosis and treatment of neurological disorders, including epilepsy, migraines, and other related conditions^[115]. Implantable neuroelectrodes can be categorized based on their functions into two main types: Recording Electrodes: These include SEEG electrodes, which capture electroencephalogram signals through deep electrodes surgically implanted within brain tissue^[37]. Stimulation Electrodes: These encompass DBS electrodes, which, following the recording of nervous system signals, provide electrical stimulation aimed at treating neurological disorders^[33].

SEEG electrodes are surgically implanted into brain tissue to record electroencephalography (EEG) signals, which reflect collective transmembrane currents from multiple neurons, as well as action potentials from individual neurons or single units^[37]. The basic dimensions of these electrodes range from 0.8 to 1.23 mm. Fiath *et al.* employed a SEEG electrode fabricated based on the PI film^[49]. This micro-cylindrical SEEG electrode, with a diameter of 800 μm , was created by depositing a metal layer, such as platinum (Pt), on its surface and employing a thin-film convolution process [Figure 13A]. However, this SEEG electrode was limited to only 32 channels, which is relatively low. Pothof *et al.* employed time-domain multiplexing (TDM), reducing the number of leads by a 16:1 ratio while increasing the number of channels to 128^[216]. TDM allows external signals measured by multiple electrodes to be used as input signals and transmitted from the same output channel, greatly compressing the position occupied by the electrode leads^[216,217] [Figure 13B and C]. Further, Steinmetz *et al.* proposed a neural pixel probe fabricated using complementary metal-oxide-semiconductor (CMOS) technology, which combines TDM with a very high integration of 1,280 channels in a single shank^[218]. In addition to the number of electrodes, the density of SEEG electrodes is also an important metric, and increasing the electrode density by decreasing the size of individual electrodes can improve the resolution of SEEG monitoring and even sense the electrical activity of a single neuron^[37]. In 2021, Gerbella *et al.* designed a neuroelectrode combining macroelectrodes and microelectrodes^[48], which saves the space occupied by the electrodes, improves the electrode density, and enhances the limit of the electrode's perceptual resolution. Recently, Liu *et al.* proposed a neural probe with an extremely high number of channels (1024)^[32], very high stability (> 105 weeks) and reusability [Figure 13D and E]. Therefore, the current mainstream research direction of SEEG electrodes is to further improve the number and density of recording sites on a single-shank probe, the recording accuracy of a single recording site, and the stability and effectiveness of long-time recording of the probe by combining multiple fabrication techniques.

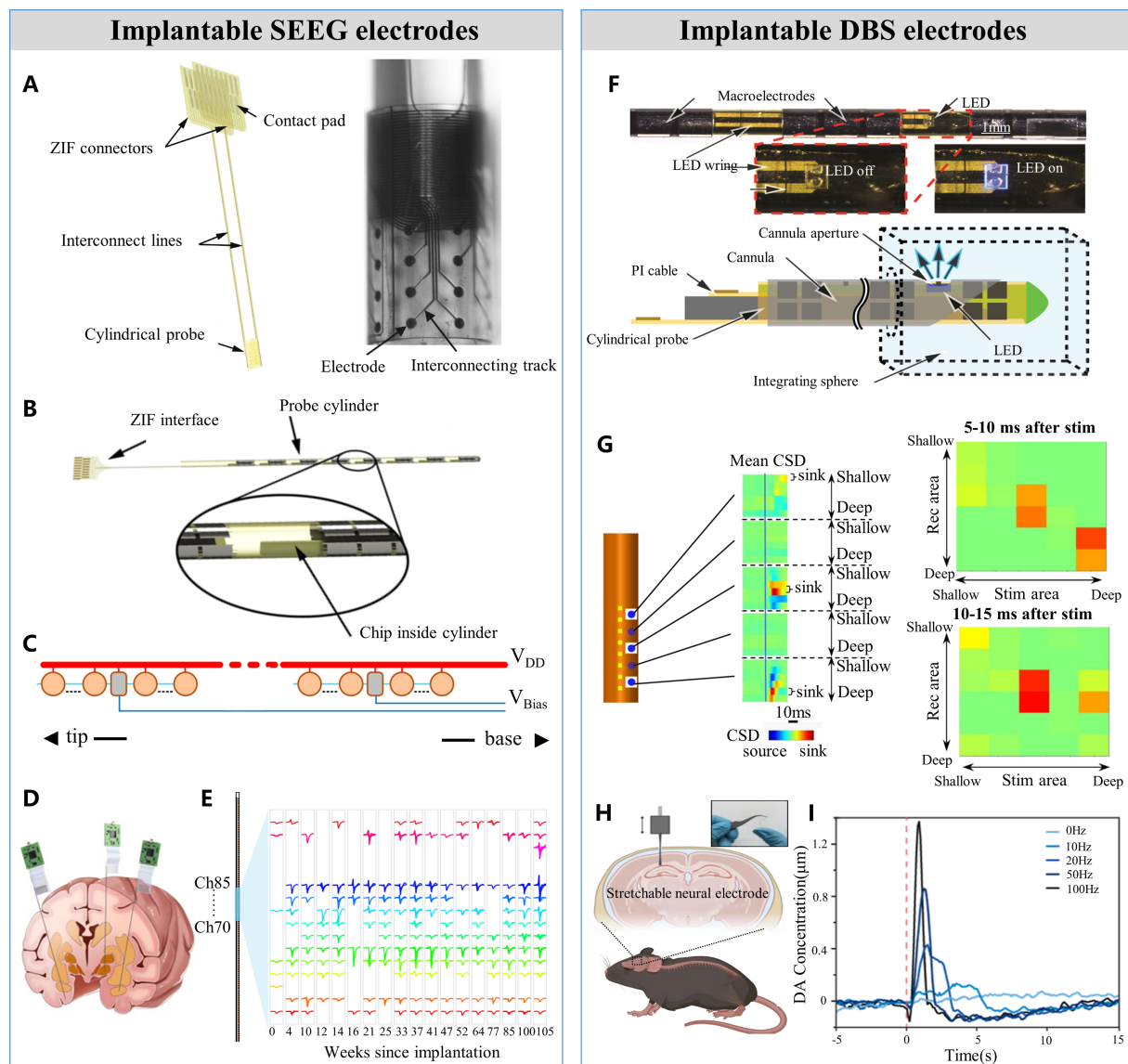


Figure 13. Structure and application of SEEG electrode and DBS electrode. (A) Basic structure of SEEG electrode. Reproduced with permission^[49]. Copyright 2018, Walter de Gruyter; (B and C) Multi-channel SEEG electrode lead integration. Reproduced with permission^[216,217]. Copyright 2015, Elsevier. Copyright 2017, Molecular Diversity Preservation International; (D) Whole-brain signal monitoring by four-handed 1024-channel SEEG electrode; (E) Multi-channel SEEG electrode prolonged whole-brain signal monitoring result sampling. Reproduced with permission^[32]. Copyright 2024, Springer Nature; (F) DBS electrodes consisting of PI cables with LEDs inserted inside the micro-cylindrical PI probes. Reproduced with permission^[105]. Copyright 2015, Elsevier; (G) Induced potential distribution within the respective depths at different times after stimulation. Reproduced with permission^[19]. Copyright 2017, John Wiley and Sons; (H) DBS electrode applied to stimulation experiments on mouse brain. Reproduced with permission^[95]. Copyright 2023, Springer Nature; (I) Signal feedback of mouse brain under different optogenetic stimulation. Reproduced with permission^[220]. Copyright 2024, American Chemical Society. SEEG: Stereo electroencephalogram; DBS: deep brain stimulation; PI: polyimide; LEDs: light-emitting diodes.

DBS electrodes, as a type of implantable neuroelectrode, can both record pathological brain activity and provide adjustable stimulation for the treatment of neurological and psychiatric disorders^[33]. The current stimulation methods utilized in DBS electrodes predominantly comprise optogenetic and chemical stimulation techniques. In the realm of optogenetic stimulation, Schwaerzle *et al.* introduced a polymer-based neural probe that incorporates an integrated light-emitting diode (LED) chip^[105]. The electrode can

deliver optical stimulation and conditioning directly to the targeted implantation site via the LED [Figure 13F]. Notably, the efficacy of optical stimulation is constrained by the inherent wavelength emission of the LED, necessitating precise modulation of parameters such as wavelength, intensity, and emission frequency to align with the therapeutic requirements at various treatment stages^[34,219]. In 2017, Tamaki *et al.* developed a neural probe equipped with eight recording sites and three light-emitting sites^[19]. This design successfully facilitated both optical stimulation and electrophysiological signal recording in rat brain experiments [Figure 13G]. As DBS electrode technology advances and exploration into novel stimulation methods continues, a broader array of techniques is emerging. In 2023, Lee *et al.* introduced a conductively stable and mechanically durable bilayer eutectic gallium indium (EGaIn) composite-coated stretchable fiber^[95], enabling both optical and electrical stimulation of neuronal cells of the mouse brain [Figure 13H]. Similarly, recently, Kim *et al.* proposed a multifunctional flexible thermally stretched fiber neural probe designed for bi-directional synapse probing within the brain^[220] [Figure 13I]. Collectively, these advancements in DBS technologies present new avenues for interrogating dysfunctional brain circuits and assessing the therapeutic potential of modulating their outputs.

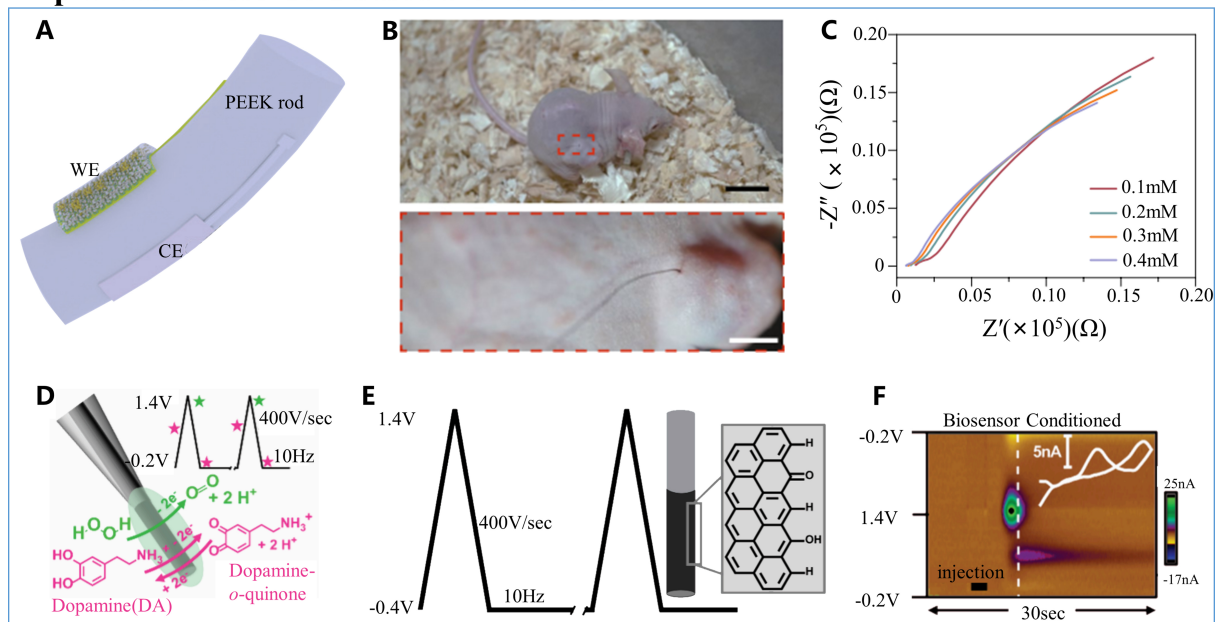
To sum up, the current selection of implantable neuroelectrode types primarily depends on the specific requirements of the application. For long-term implantation, the stability of the electrode material and structure over time must be carefully assessed through extensive animal and clinical studies. Additionally, there is a growing trend towards the development of multifunctional neuroelectrodes that combine recording and stimulation capabilities. Future efforts should concentrate on reducing electrode size through reliable and high-precision manufacturing processes. Smaller electrodes result in smaller incisions and less post-operative pain for patients, promoting greater acceptance of surgical interventions.

Implantable cylindrical biosensors

Implantable biosensors are sensors that utilize materials sensitive to biological substances and physiological signals for the detection of biological organisms by implanting sensors into the human body^[24]. These biosensors play a crucial role in providing *in vivo* sensing capabilities, expanding the integration and application of sensors in medical devices. There are two main categories of biosensors based on the information they detect: implantable biosensors that focus on detecting biomarkers such as glucose sensors^[12,221], calcium sensors^[11], and neurotransmitter sensors^[222]; and implantable biosensors that focus on detecting both electrophysiological signals of the organism and biochemical signals, such as temperature sensors, pH sensors, and intracranial pressure sensors^[223-225].

Biosensors focusing on the detection of biomarkers have biosensitive materials as recognition elements, which mainly consist of appropriate physicochemical transducers and signal amplification devices. In 2018, Pu *et al.* proposed a cylindrical enzyme electrode glucose biosensor fabricated by inkjet printing^[12] [Figure 14A]. *In vivo* experiments in rats demonstrated that the sensor has the potential to be used for subcutaneous tissue implantation for continuous glucose monitoring. In 2020, Wang *et al.* suggested that functionalized MWCNTs twisted into helical fiber bundles could be utilized to detect changes in calcium ion and glucose concentrations in the blood, as well as hydrogen peroxide (H₂O₂) concentration and distribution^[11] [Figure 14B and C]. A continuous blood glucose monitoring system comprising a plastic optical fiber, a diboronic acid receptor-based chemical indicator, reinforcing wires, and thermocouples enables direct measurement of plasma glucose concentration within the patient's blood vessels^[226]. Furthermore, the immobilization of glucose oxidase (GOx) on the surface of carbon fibers enabled the micro-cylindrical electrode to simultaneously monitor glucose and dopamine *in vivo*^[227] [Figure 14D-F]. The sensor demonstrated high sensitivity and selectivity, positioning it as a promising tool for reliable metabolic studies and neurotransmitter monitoring.

Implantable biosensors based biomarkers



Implantable biosensors based electrophysiological and biochemical signals

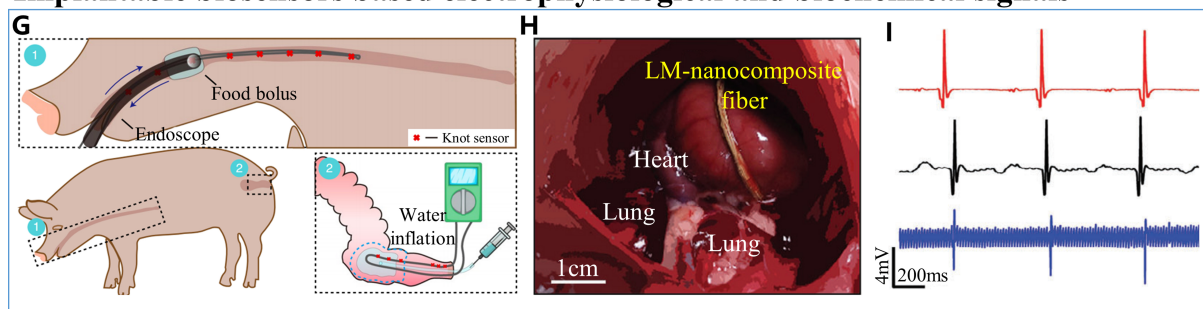


Figure 14. Applications of Typical Implantable Biosensors. (A) Structure of an implantable glucose/blood glucose sensor. Reproduced with permission^[12]. Copyright 2018, Lab on a Chip; (B) Detection of tumor growth utilizing H_2O_2 as a biomarker; (C) Sensitive response of an H_2O_2 sensor to ultra-low concentrations of H_2O_2 . Reproduced with permission^[11]. Copyright 2019, Springer Nature; (D) Principle of identification and quantification of DA (pink) and H_2O_2 (green) on the micro-cylindrical biosensor surface; (E) Electrochemical modification of carbon fibers to immobilize oxidase on their surface; (F) Resultant graph of glucose and DA detected in a benchtop flow cell. Reproduced with permission^[227]. Copyright 2024, American Chemical Society; (G) Schematic depiction of esophageal and rectoanal pressure measurements using a porcine model. Reproduced with permission^[228]. Copyright 2022, Springer Nature; (H) Application of cardiac beat sensors in the detection of cardiovascular health; (I) Cardiac beat sensor for monitoring epicardial electrograms. Reproduced with permission^[229]. Copyright 2024, John Wiley and Sons. DA: dopamine.

Biosensors primarily detect electrophysiological and biochemical signals of biological. These sensors were used for monitoring intracranial pressure, PH level, temperature, and more. In 2016, Musolino *et al.* proposed an optical fiber temperature sensor based on rare-earth-doped tellurite glass, integrated at the tip of a conventional silica optical fiber^[224]. This innovative design enables long-term *in vivo* temperature measurements. Additionally, a piezoresistive pressure sensor catheter, constructed by injecting liquid metal into a silicone tube, was successfully employed to monitor gastrointestinal dynamic data in anesthetized pigs^[228] [Figure 14G]. Recently, Nam *et al.* proposed a stretchable microfiber composed of a phase-converted liquid metal core and a multifunctional nanocomposite shell^[229]. In rat muscle implantation experiments, the fibers successfully sensed muscle movements and converted them into electrical signals for further analysis [Figure 14H and I]. While current implantable biosensors have demonstrated a wide range of applications in sensing and monitoring, the long-term reliability of these biosensors and the biochemical

effects of prolonged implantation in living organisms have been inadequately addressed in existing studies. Therefore, further research is essential to evaluate these aspects comprehensively.

Interventional MRI resonant markers

MRI provides 3D visual imaging of the anatomy and surrounding tissues of the human body. The technique exploits the magnetization and spin alignment of hydrogen nuclei in a strong magnetic field, where an applied RF pulse alters their spin, and the resulting emitted signal is detected and processed to generate an image^[116,230]. The operation process^[231] is shown in [Figure 15A](#). Compared to other medical imaging modalities, such as X-ray imaging, MRI offers several advantages, including the absence of ionizing radiation, superior soft tissue contrast, and the capability of producing unique three-dimensional images.

In interventional procedures, MRI markers are typically placed on the tips of surgical instruments or catheters to monitor and visualize their positions. Based on their operational principles, MRI markers are generally classified into three modalities: passive, active, and resonant. Passive methods involve coating or embedding paramagnetic particles into the tip of the device. For instance, a gadolinium-filled balloon MRI catheter has been utilized for procedures such as transfemoral right heart catheterization^[232] and transcatheter cavopulmonary anastomosis and shunt^[233] [[Figure 15B](#)]. In addition to paramagnetic particles, special braided metal structures have been employed for passive MRI labeling^[234]. While this approach is simple and efficient, it is subject to uncertainties, such as tissue inhomogeneity within the body affecting position determination.

Active MRI markers use coaxial cables to connect an external magnetic resonance (MR) scanner to a receiving coil at the instrument tip, which can be powered either by the scanner or a direct current (DC) power supply^[235]. Saikus *et al.* developed an active MRI probe utilizing coil winding and demonstrated its application in jugular vein access in healthy pigs^[236] [[Figure 15C](#)]. To address the need for high customization and improve manufacturing efficiency, Yildirim *et al.* designed a series of active MRI markers using inkjet printing technology^[39,85]. This active method generates a locally enhanced magnetic field, providing excellent visualization. However, the use of coaxial cables can occupy valuable cavity space and may lead to induced RF heating. To address this challenge, an acousto-optic labeling-based MRI tracking technique has been developed^[117]. This approach integrates piezoelectric crystals with fiber Bragg gratings to mitigate the risk of RF-induced heating [[Figure 15D](#)], offering a novel solution for employing active MRI markers in catheter detection.

In contrast, MRI marking (also known as semi-active) methods based on wireless resonant circuits ensure good imaging without the risk of RF heating^[13,99,117]. In this approach, the RF circuit, comprising an RF coil and a capacitor, is tuned to resonate at the Larmor frequency^[237,238]. Ellersiek *et al.* developed a flexible MRI marker comprising six winding coils and adjustable capacitors on a PI film with a thickness of less than 50 μm using a MEMS method^[239] [[Figure 15E](#)]. Additionally, a low-profile RF resonance marker was fabricated directly on a guiding catheter surface using physical vapor deposition and electroplating processes^[47]. In addition, several novel sensing principles for interventional MRI markers have been applied to *in vivo* real-time imaging. Bilgin *et al.* designed a self-resonant RF sensor capable of remote *in-situ* temperature sensing during real-time interventional MRI^[45]. The effectiveness of this sensor was experimentally demonstrated by manually operating the catheter tip inside an *ex vivo* porcine kidney [[Figure 15F](#)]. In conclusion, numerous studies have demonstrated the potential of resonance-based MRI markers for providing effective and safe imaging guidance during minimally invasive surgical interventions.

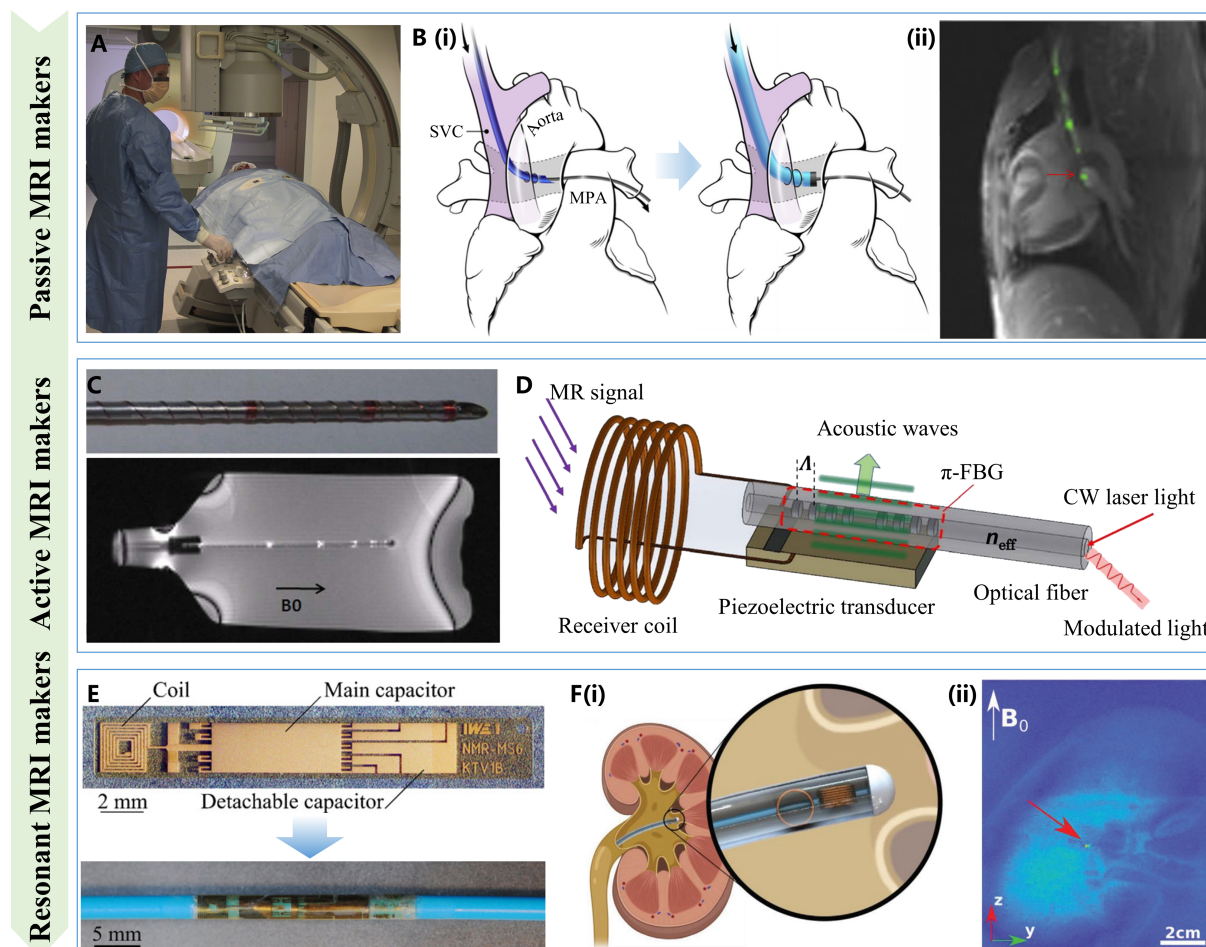


Figure 15. Interventional MRI markers and their applications. (A) Diagram of an interventional MRI real-time guided surgical intervention procedure. Reproduced with permission^[231]. Copyright 2015, Elsevier; (B) Diagram (i) and real-time imaging (ii) of a needle (dark blue) as well as a long introducer sheath (light blue) advanced from the superior vena cava (SVC) (purple) to the main pulmonary artery (MPA) during passive MRI guidance. Reproduced with permission^[233]. Copyright 2016, Elsevier; (C) An active MRI probe utilizing coil winding (top and middle) and an active MRI needle for *in vitro* visualization imaging (bottom). Reproduced with permission^[236]. Copyright 2011, John Wiley and Sons; (D) Illustration of acousto-optic markers. Reproduced with permission^[117]. Copyright 2020, John Wiley and Sons; (E) Images of MR tracking devices prepared on PI films, shown both completed (top) and conformally affixed to the catheter (bottom). Reproduced with permission^[239]. Copyright 2010, Elsevier; (F) Schematic of an RF sensor with MRI coil coupling integrated into the catheter tip and implanted into a porcine kidney (i), and a demonstration of the MRI experiment with the manually operated catheter tip inside an isolated porcine kidney (ii). Reproduced with permission^[45]. Copyright 2022, John Wiley and Sons. MRI: Magnetic resonance imaging; SVC: superior vena cava; MPA: main pulmonary artery; MR: magnetic resonance; PI: polyimide; RF: radiofrequency.

CONCLUSION AND OUTLOOK

Micro-cylindrical and fibric electronics have demonstrated significant application potential in various domains, including wearable devices, biomedicine, and environmental monitoring. This is attributed to their unique shape, featuring a large aspect ratio and superior mechanical properties. In this review, we provide a comprehensive analysis of the primary fabrication methods for micro-cylindrical or fibric workpieces. We thoroughly discuss the critical characteristics of existing fabrication technologies and their typical applications in the development of micro-cylindrical or fibric electronics. Chemical coating and electroplating techniques offer good coverage and adhesion but relatively low precision, making them suitable for integrated fiber-based sensors, which have already found applications in wearable fabrics. Rotational lithography, while providing high precision, is costly and is predominantly employed in the

manufacturing of surgical instruments and implantable bioelectronics. Printing technologies, characterized by their adaptability and compatibility with conformal manufacturing processes, remain in an emerging stage of research. These technologies require further investigation to improve material compatibility and precision. Although nanoimprint and laser processing technologies are relatively mature, their applications in micro-cylindrical electronic devices are limited and necessitate further exploration. Selecting the appropriate fabrication technology is crucial for specific structures and applications of micro-cylindrical or fiber-based devices. Despite advancements in fabrication techniques driving innovations and expansions in fields such as wearable electronics, surgical robots, and implantable electronics, several significant challenges persist for practical industrial applications. These challenges include achieving efficient high-precision manufacturing, ensuring the biocompatibility of material systems, maintaining stability for long-term wear or implantation, enabling system-level integration, and advancing intelligent applications.

(1) Efficient high-precision manufacturing. Micro-cylindrical surfaces, particularly fibers with diameters in the hundreds of micrometers, exhibit ultra-high curvature, necessitating highly precise surface patterning techniques. While rotational lithography and high-precision printing techniques show promise for achieving high precision, challenges such as high-precision alignment during the rotation of micro-cylindrical substrates must be addressed. Furthermore, the industrial application of micro-cylindrical devices requires standardized and efficient manufacturing processes to enhance device consistency and reliability.

(2) Biocompatibility of material systems. In medical and wearable applications, fibric electronics must be evaluated for biocompatibility to avoid adverse biological reactions. It is essential to avoid the use of highly chemically reactive metals or compounds as electrodes or sensitive layers. For implantable devices, special attention must be paid to matching the modulus of the device structure with biological tissues, utilizing substrates with lower modulus to mitigate damage to tissue cells.

(3) Stability for long-term wear/implantation. Micro-cylindrical electronic devices must fulfill stringent short-term safety requirements for interventional surgeries while also ensuring long-term reliability for wearable applications. Additionally, these devices must maintain stability as implantable electrodes or biosensors within the body. Overcoming physical failures due to friction and fatigue, as well as chemical failures resulting from material oxidation and decomposition, is crucial for ensuring long-term stability and functionality.

(4) System-level integration. Integrated sensing systems are vital for practical applications. Key issues include ensuring self-powering and wireless transmission for wearable sensing systems and addressing crosstalk and decoupling in multi-mode sensing. Successful system-level integration involves incorporating sensors, inductors, capacitors, resistors, and transistors onto fiber-based devices to create comprehensive and functional sensing systems.

(5) Intelligent applications. With the rapid development of the Internet of Things (IoT) and artificial intelligence (AI), micro-cylindrical electronic devices must incorporate more intelligent functions to expand their application fields and enhance user convenience. For instance, in wearable devices, sensors must not only monitor physiological parameters in real time but also process data and provide intelligent feedback. By leveraging machine learning algorithms, these sensors can achieve more precise health monitoring and disease prediction, thereby improving user experience and application value. In the medical field, surgical robots equipped with micro-cylindrical sensors can facilitate more precise operations by providing real-time monitoring of various parameters during surgery, thereby enhancing safety and outcomes.

The fabrication technology of micro-cylindrical electronic devices is anticipated to advance towards higher precision, reduced costs, enhanced material compatibility, and improved efficiency. The introduction of novel materials and process improvements is expected to overcome existing technical bottlenecks, such as the integration of flexible electronic materials and nanomaterials. Furthermore, as technology progresses, micro-cylindrical devices will exhibit significant potential in emerging fields, including wearable devices, smart healthcare, and environmental monitoring. Interdisciplinary integration will further propel the development of this field, offering more innovative solutions for practical applications.

DECLARATIONS

Authors' contributions

Conducted the literature review, outlined the manuscript structure, and wrote the manuscript draft: Wang H, Wu H, Zhao C, Wu Q, Wang S, Zhang Z

Participated in the discussion of the review content: Zeng M, Wei H, Ye D

Initiated the reviewing idea and were involved in the discussion and revision of the manuscript: Wang H, Wu H, Ye D, Huang Y

All authors have read the manuscript and approved the final version.

Availability of data and materials

Not applicable.

Financial support and sponsorship

This study was supported by the National Key Research and Development Program of China (2021YFB3200703) and the National Natural Science Foundation of China (Grant Nos. 52175537, 52188102).

Conflicts of interest

Huang Y is the Editor-in-Chief of the journal *Soft Science*, while the other authors have declared that they have no conflicts of interest.

Ethical approval and consent to participate

Not applicable.

Consent for publication

Not applicable.

Copyright

© The Author(s) 2024.

REFERENCES

1. Zheng Y, Wang Z, Chen P, Peng H. Semiconductor fibers for textile integrated electronic systems. *Natl Sci Rev* 2024;11:nwae143. DOI PubMed PMC
2. Park J, Jeong Y, Kim J, Gu J, Wang J, Park I. Biopsy needle integrated with multi-modal physical/chemical sensor array. *Biosens Bioelectron* 2020;148:111822. DOI
3. Yu D, Qian Q, Wei L, et al. Emergence of fiber supercapacitors. *Chem Soc Rev* 2015;44:647-62. DOI
4. Khan AQ, Shafiq M, Li J, et al. Recent developments in artificial spider silk and functional gel fibers. *SmartMat* 2023;4:e1189. DOI
5. Cai J, Du M, Li Z. Flexible temperature sensors constructed with fiber materials. *Adv Mater Technol* 2022;7:2101182. DOI
6. Wu Y, Dong S, Li X, et al. A stretchable all-nanofiber iontronic pressure sensor. *Soft Sci* 2023;3:33. DOI
7. Li X, Zhang S, Li K, et al. Electrospun micro/nanofiber-based biomechanical sensors. *ACS Appl Polym Mater* 2023;5:6720-46. DOI
8. Cui X, Wu H, Wang R. Fibrous triboelectric nanogenerators: fabrication, integration, and application. *J Mater Chem A* 2022;10:15881-905. DOI

9. Zhong Y, Liang Q, Chen Z, et al. High-performance fiber-shaped vertical organic electrochemical transistors patterned by surface photolithography. *Chem Mater* 2023;35:9739-46. DOI
10. Wu F, Lan B, Cheng Y, et al. A stretchable and helically structured fiber nanogenerator for multifunctional electronic textiles. *Nano Energy* 2022;101:107588. DOI
11. Wang L, Xie S, Wang Z, et al. Functionalized helical fibre bundles of carbon nanotubes as electrochemical sensors for long-term in vivo monitoring of multiple disease biomarkers. *Nat Biomed Eng* 2020;4:159-71. DOI
12. Pu Z, Tu J, Han R, et al. A flexible enzyme-electrode sensor with cylindrical working electrode modified with a 3D nanostructure for implantable continuous glucose monitoring. *Lab Chip* 2018;18:3570-7. DOI
13. Jordan CD, Thorne BRH, Wadhwa A, et al. Wireless resonant circuits printed using aerosol jet deposition for MRI catheter tracking. *IEEE Trans Biomed Eng* 2020;67:876-82. DOI PubMed PMC
14. Peng Z, Wang M, Lv H, et al. Electric field-driven microscale 3D printing of flexible thin-walled tubular mesh structures of molten polymers. *Materi Design* 2023;225:111433. DOI
15. Zhang C, Zhang L, Pu Z, Bao B, Ouyang W, Li D. Fabricating 1D stretchable fiber-shaped electronics based on inkjet printing technology for wearable applications. *Nano Energy* 2023;113:108574. DOI
16. Jose M, Bezerra Alexandre E, Neumaier L, et al. Future thread: printing electronics on fibers. *ACS Appl Mater Interfaces* 2024;16:7996-8005. DOI
17. Horiuchi T, Suzuki Y. Fabrication of fine and high-density multithread spirals on inner surfaces of small-diameter pipes using laser scan lithography. *Jpn J Appl Phys* 2014;53:06JM10. DOI
18. Hwang S, Kang M, Lee A, et al. Integration of multiple electronic components on a microfibre towards an emerging electronic textile platform. *Nat Commun* 2022;13:3173. DOI PubMed PMC
19. Tamaki S, Matsunaga T, Kuki T, Mushiaki H, Furusawa Y, Haga Y. Neural probe with multiple optical stimulation in depth direction. *Electron Commun Jpn* 2017;100:45-54. DOI
20. Ham S, Kang M, Jang S, et al. One-dimensional organic artificial multi-synapses enabling electronic textile neural network for wearable neuromorphic applications. *Sci Adv* 2020;6:eaba1178. DOI PubMed PMC
21. Fabiano S, Facchetti A. Stretchable helix-structured fibre electronics. *Nat Electron* 2021;4:864-5. DOI
22. Wang Q, Han W, Wang Y, Lu M, Dong L. Tape nanolithography: a rapid and simple method for fabricating flexible, wearable nanophotonic devices. *Microsyst Nanoeng* 2018;4:31. DOI PubMed PMC
23. Ye C, Zhao L, Yang S, Li X. Recent research on preparation and application of smart joule heating fabrics. *Small* 2024;20:e2309027. DOI
24. Park J, Seo B, Jeong Y, Park I. A review of recent advancements in sensor-integrated medical tools. *Adv Sci* 2024;11:e2307427. DOI PubMed PMC
25. Paulk AC, Kfir Y, Khanna AR, et al. Large-scale neural recordings with single neuron resolution using Neuropixels probes in human cortex. *Nat Neurosci* 2022;25:252-63. DOI
26. Liu J, Tian G, Yang W, Deng W. Recent progress in flexible piezoelectric devices toward human-machine interactions. *Soft Sci* 2022;2:22. DOI
27. Wang P, Li X, Sun G, et al. Natural human skin-inspired wearable and breathable nanofiber-based sensors with excellent thermal management functionality. *Adv Fiber Mater* 2024. DOI
28. Sun X, Zhang F, Zhang L, et al. Enhanced electromechanical conversion via in situ grown CsPbBr₃ nanoparticles/poly(vinylidene fluoride) fibers for physiological signal monitoring. *Soft Sci* 2022;2:1. DOI
29. Zhang C, Ouyang W, Zhang L, Li D. A dual-mode fiber-shaped flexible capacitive strain sensor fabricated by direct ink writing technology for wearable and implantable health monitoring applications. *Microsyst Nanoeng* 2023;9:158. DOI PubMed PMC
30. Zhang M, Su H, Zhang C, Sun Z, Jiang Z. Smart optical fiber fabric based on side-emitting and side-coupling for pulse and blood oxygen measurement. *Text Res J* 2023;93:3382-92. DOI
31. Tian S, Wang Y, Deng H, Wang Y, Zhang X. Flexible pressure and temperature sensors towards e-skin: material, mechanism, structure and fabrication. *Soft Sci* 2023;3:30. DOI
32. Liu Y, Jia H, Sun H, et al. A high-density 1,024-channel probe for brain-wide recordings in non-human primates. *Nat Neurosci* 2024;27:1620-31. DOI
33. Lozano AM, Lipsman N, Bergman H, et al. Deep brain stimulation: current challenges and future directions. *Nat Rev Neurol* 2019;15:148-60. DOI PubMed PMC
34. Nazempour R, Zhang B, Ye Z, Yin L, Lv X, Sheng X. Emerging applications of optical fiber-based devices for brain research. *Adv Fiber Mater* 2022;4:24-42. DOI
35. Sellers KK, Chung JE, Zhou J, et al. Thin-film microfabrication and intraoperative testing of μ ECoG and iEEG depth arrays for sense and stimulation. *J Neural Eng* 2021;18:045014. DOI PubMed PMC
36. Huang S, He M, Yao C, et al. Petromyzontidae-biomimetic multimodal microneedles-integrated bioelectronic catheters for theranostic endoscopic surgery. *Adv Funct Mater* 2023;33:2214485. DOI
37. Hong G, Lieber CM. Novel electrode technologies for neural recordings. *Nat Rev Neurosci* 2019;20:330-45. DOI PubMed PMC
38. Wang Z, Wu T, Wang Z, et al. Designer patterned functional fibers via direct imprinting in thermal drawing. *Nat Commun* 2020;11:3842. DOI PubMed PMC
39. Uzun D, Yildirim DK, Bruce CG, et al. Interventional device tracking under MRI via alternating current controlled inhomogeneities.

- Magn Reson Med* 2024;92:346-60. DOI PubMed PMC
40. Yang Z, Shi J, Sun B, Yao J, Ding G, Sawada R. Fabrication of electromagnetically-driven tilted microcoil on polyimide capillary surface for potential single-fiber endoscope scanner application. *Micromachines* 2018;9:61. DOI PubMed PMC
 41. Huang F, Hu J, Yan X, Meng F. High-linearity, ultralow-detection-limit, and rapid-response strain sensing yarn for data gloves. *J Ind Text* 2022;51:4554S-70S. DOI
 42. Kara G, Bolat S, Sharma K, et al. Conformal integration of an inkjet-printed PbS QDs-graphene IR photodetector on a polymer optical fiber. *Adv Mater Technol* 2023;8:2201922. DOI
 43. Kwon S, Hwang YH, Nam M, et al. Recent progress of fiber shaped lighting devices for smart display applications - a fibertronic perspective. *Adv Mater* 2020;32:e1903488. DOI PubMed
 44. Lee K, Paulk AC, Ro YG, et al. Flexible, scalable, high channel count stereo-electrode for recording in the human brain. *Nat Commun* 2024;15:218. DOI PubMed PMC
 45. Bilgin MB, Tiryaki ME, Lazovic J, Sitti M. Radio frequency sensing-based in situ temperature measurements during magnetic resonance imaging interventional procedures. *Adv Mater Technol* 2022;7:2101625. DOI
 46. Yun J, Kim HW, Kim H, Lee J. Electrical impedance spectroscopy on a needle for safer Veress needle insertion during laparoscopic surgery. *Sensor Actuat B Chem* 2017;250:453-60. DOI
 47. Baysoy E, Yildirim DK, Ozsoy C, Mutlu S, Kocaturk O. Thin film based semi-active resonant marker design for low profile interventional cardiovascular MRI devices. *MAGMA* 2017;30:93-101. DOI PubMed
 48. Gerbella M, Borra E, Pothof F, et al. Histological assessment of a chronically implanted cylindrically-shaped, polymer-based neural probe in the monkey. *J Neural Eng* 2021;18:024001. DOI
 49. Fiáth R, Hofer KT, Csikós V, et al. Long-term recording performance and biocompatibility of chronically implanted cylindrically-shaped, polymer-based neural interfaces. *Biomed Tech* 2018;63:301-15. DOI
 50. Hayat S, Basir A, Yoo H. Modeling and in vitro measurement of a compact antenna for intravascular catheter tracking and imaging system. *IEEE Trans Instrum Meas* 2023;72:1-14. DOI
 51. Yun J, Kim HW, Lee JH. Improvement of depth profiling into biotissues using micro electrical impedance spectroscopy on a needle with selective passivation. *Sensors* 2016;16:2207. DOI PubMed PMC
 52. Ganesana M, Trikantopoulos E, Maniar Y, Lee ST, Venton BJ. Development of a novel micro biosensor for in vivo monitoring of glutamate release in the brain. *Biosens Bioelectron* 2019;130:103-9. DOI PubMed PMC
 53. Zhang R, Wang X, Cai S, Tao K, Xu Y. A solid-state wire-shaped supercapacitor based on nylon/Ag/polypyrrole and nylon/Ag/MnO₂ electrodes. *Polymers* 2023;15:1627. DOI PubMed PMC
 54. Zhao Y, Lin Z, Dong S, Chen M. Review of wearable optical fiber sensors: drawing a blueprint for human health monitoring. *Opt Laser Technol* 2023;161:109227. DOI
 55. Dong Y, Tian Y, Yang Y, et al. Multiple covalent modification enables nylon fiber biosensor with robust scrub-resistant and signal-capture ability for multisenario health monitoring and security warning. *Int J Biol Macromol* 2024;281:136518. DOI
 56. Wang Z, Xing D, Yin R, et al. Breathable and waterproof conductive cotton fabric pressure sensor with distinguished electrothermal and electromagnetic interference shielding performances. *Appl Mater Today* 2024;38:102256. DOI
 57. Wang S, Xu Q, Sun H. Functionalization of fiber devices: materials, preparations and applications. *Adv Fiber Mater* 2022;4:324-41. DOI
 58. Sheng F, Zhao C, Zhang B, Tan Y, Dong K. Flourishing electronic textiles towards pervasive, personalized and intelligent healthcare. *Soft Sci* 2024;4:2. DOI
 59. Liu T, He Z, Liu H, et al. Heat-resistant and high-performance solid-state supercapacitors based on poly(*para*-phenylene terephthalamide) fibers via polymer-assisted metal deposition. *ACS Appl Mater Interfaces* 2021;13:18100-9. DOI PubMed
 60. Ge J, Sun L, Zhang FR, et al. A stretchable electronic fabric artificial skin with pressure-, lateral strain-, and flexion-sensitive properties. *Adv Mater* 2016;28:722-8. DOI PubMed
 61. Yang Z, Deng J, Chen X, Ren J, Peng H. A highly stretchable, fiber-shaped supercapacitor. *Angew Chem Int Ed Engl* 2013;52:13453-7. DOI PubMed
 62. Wang Y, Ding Y, Guo X, Yu G. Conductive polymers for stretchable supercapacitors. *Nano Res* 2019;12:1978-87. DOI
 63. Xu W, Luo J, Zhang W, et al. Flexible airflow-strain dual response sensor with high sensitivity based on polyurethane conductive fiber flocced carbon fibers. *J Mater Sci Mater Electron* 2024;35:13443. DOI
 64. Li P, Liu J, Wang S, et al. Highly stretchable electromechanical sensors with ionotronic knots based on hydrogel fibers. *Adv Mater Technol* 2024;9:2302202. DOI
 65. Ding H, Wu Z, Wang H, et al. An ultrastretchable, high-performance, and crosstalk-free proximity and pressure bimodal sensor based on ionic hydrogel fibers for human-machine interfaces. *Mater Horiz* 2022;9:1935-46. DOI
 66. Niu Q, Huang L, Fan S, Yao X, Zhang Y. 3D printing silk fibroin/polyacrylamide triple-network composite hydrogels with stretchability, conductivity, and strain-sensing ability as bionic electronic skins. *ACS Biomater Sci Eng* 2024;10:3489-99. DOI
 67. Yin Z, Jian M, Wang C, et al. Splash-resistant and light-weight silk-sheathed wires for textile electronics. *Nano Lett* 2018;18:7085-91. DOI
 68. Li C, Guo C, Fitzpatrick V, et al. Design of biodegradable, implantable devices towards clinical translation. *Nat Rev Mater* 2020;5:61-81. DOI
 69. Kwon CH, Ko Y, Shin D, et al. High-power hybrid biofuel cells using layer-by-layer assembled glucose oxidase-coated metallic

- cotton fibers. *Nat Commun* 2018;9:4479. DOI PubMed PMC
70. Chen C, Feng J, Li J, Guo Y, Shi X, Peng H. Functional fiber materials to smart fiber devices. *Chem Rev* 2023;123:613-62. DOI
71. Xiao R, Yu G, Xu BB, Wang N, Liu X. Fiber surface/interfacial engineering on wearable electronics. *Small* 2021;17:e2102903. DOI PubMed
72. Li WJ, Mai JD, Ho C. Sensors and actuators on non-planar substrates. *Sensor Actuat A Phys* 1999;73:80-8. DOI
73. Goto S, Matsunaga T, Chen JJ, Makishi W, Esashi M, Haga Y. Fabrication techniques for multilayer metalization and patterning, and surface mounting of components on cylindrical substrates for tube-shaped micro-tools. In: 2006 International Conference on Microtechnologies in Medicine and Biology; 2006 May 09-12; Okinawa, Japan. IEEE; 2006. pp. 217-20. DOI
74. de Miranda R, Zamponi C, Quandt E. Rotational UV lithography device for cylindrical substrate exposure. *Rev Sci Instrum* 2009;80:015103. DOI PubMed
75. Joshima Y, Kokubo T, Horiuchi T. Application of laser scan lithography to fabrication of microcylindrical parts. *Jpn J Appl Phys* 2004;43:4031. DOI
76. Horiuchi T, Suzuki Y. Micro-fabrication of air-bearing grooves onto inner surfaces of fine copper pipes. *Microelect Eng* 2013;110:422-6. DOI
77. Horiuchi T, Sasaki R. New laser-scan exposure system for delineating precise helical patterns onto sub-50- μ m wires. *Jpn J Appl Phys* 2012;51:06FL01. DOI
78. Horiuchi T, Fujii H, Yasunaga K. Lithography onto surfaces of fine-diameter pipes using rotary scan-projection exposure. *J Photopol Sci Technol* 2015;28:273-8. DOI
79. Doll PW, Doll C, Käßer L, et al. Rotational UV-lithography using flexible chromium-coated polymer masks for the fabrication of microstructured dental implant surfaces: a proof of concept. *J Micromech Microeng* 2020;30:045008. DOI
80. Park J, Fujita H, Kim B. Fabrication of metallic microstructure on curved substrate by optical soft lithography and copper electroplating. *Sensor Actuat A Phys* 2011;168:105-11. DOI
81. Yang Z, Zhang Y, Itoh T, Maeda R. New fabrication method of three-electrode system on cylindrical capillary surface as a flexible implantable microneedle. *Surf Rev Lett* 2013;20:1350027. DOI
82. Haga Y, Muryari Y, Goto S, Matsunaga T, Esashi M. Development of minimally invasive medical tools using laser processing on cylindrical substrates. *Electr Eng Jpn* 2011;176:65-74. DOI
83. Liao M, Wang C, Hong Y, et al. Industrial scale production of fibre batteries by a solution-extrusion method. *Nat Nanotechnol* 2022;17:372-7. DOI
84. Xie Y, Lu L, Tang Y, et al. Hierarchically nanostructured carbon fiber-nickel-carbon nanotubes for high-performance supercapacitor electrodes. *Mater Lett* 2017;186:70-3. DOI
85. Yildirim DK, Bruce C, Uzun D, et al. A 20-gauge active needle design with thin-film printed circuitry for interventional MRI at 0.55T. *Magn Reson Med* 2021;86:1786-801. DOI PubMed PMC
86. Zulkifli NA, Jeong W, Kim M, et al. 3D-printed magnetic-based air pressure sensor for continuous respiration monitoring and breathing rehabilitation. *Soft Sci* 2024;4:20. DOI
87. Zeng Y, Chen G, Zhao F, et al. 3D printing of high-temperature thick film platinum resistance temperature detector array. *Addit Manuf* 2023;73:103654. DOI
88. Chen G, Zeng Y, Zhao F, et al. Conformal fabrication of functional polymer-derived ceramics thin films. *Surf Coat Technol* 2023;464:129536. DOI
89. Fang B, Yan J, Chang D, et al. Scalable production of ultrafine polyaniline fibres for tactile organic electrochemical transistors. *Nat Commun* 2022;13:2101. DOI PubMed PMC
90. Zhang G, Lan H, Qian L, Zhao J, Wang F. A microscale 3D printing based on the electric-field-driven jet. *3D Print Addit Manuf* 2020;7:37-44. DOI PubMed PMC
91. Hobbie HA, Doherty JL, Smith BN, Maccarini P, Franklin AD. Conformal printed electronics on flexible substrates and inflatable catheters using lathe-based aerosol jet printing. *Npj Flex Electron* 2024;8:54. DOI PubMed PMC
92. Wang K, Wang X, Wang C, et al. Customizable and scalable manufacture of aesthetic ionic conductive silk yarns for e-textile devices. *Chem Eng J* 2024;487:150645. DOI
93. Fu L, Liu Y, Liu Z, et al. Carbon nanotubes coated with alumina as gate dielectrics of field-effect transistors. *Adv Mater* 2006;18:181-5. DOI
94. Carey T, Maughan J, Doolan L, et al. Knot architecture for biocompatible and semiconducting 2D electronic fiber transistors. *Small Methods* 2024;8:e2301654. DOI
95. Lee GH, Lee DH, Jeon W, et al. Conductance stable and mechanically durable bi-layer EGaIn composite-coated stretchable fiber for 1D bioelectronics. *Nat Commun* 2023;14:4173. DOI PubMed PMC
96. Woo S, Kim H, Kim J, Ryu H, Lee J. Fiber-based flexible ionic diode with high robustness and rectifying performance: toward electronic textile circuits. *Adv Elect Mater* 2024;10:2300653. DOI
97. Liao M, Wang J, Ye L, et al. A high-capacity aqueous zinc-ion battery fiber with air-recharging capability. *J Mater Chem A* 2021;9:6811-8. DOI
98. Han J, Xu C, Zhang J, et al. Multifunctional coaxial energy fiber toward energy harvesting, storage, and utilization. *ACS Nano* 2021;15:1597-607. DOI
99. Cheung CL, Wu M, Fang G, et al. Omnidirectional monolithic marker for intra-operative MR-based positional sensing in closed

- MRI. *IEEE Trans Med Imaging* 2024;43:439-48. DOI
100. Wasylczyk P, Ozimek F, Tiwari MK, Cruz Ld, Bergeles C. Bio-compatible piezoresistive pressure sensing skin sleeve for millimetre-scale flexible robots: design, manufacturing and pitfalls. In: 2019 41st Annual International Conference of the IEEE Engineering in Medicine and Biology Society (EMBC); 2019 Jul 23-27; Berlin, Germany. IEEE; 2019. pp. 1657-61. DOI
 101. Yang Z, Zhang Y, Itoh T, Maeda R. A novel MEMS compatible lab-on-a-tube technology. *Lab Chip* 2014;14:4604-8. DOI
 102. Detert M, Friesecke S, Deckert M, Rose G, Schmidt B, Kaiser M. Using the hot embossing technology for the realization of microtechnical structures in medical imaging. *Biomed Tech* 2012;57:599-602. DOI
 103. Pothof F, Galchev T, Patel M, Herbawi AS, Paul O, Ruther P. 128-Channel deep brain recording probe with heterogeneously integrated analog CMOS readout for focal epilepsy localization. In: 2015 Transducers - 2015 18th International Conference on Solid-State Sensors, Actuators and Microsystems (TRANSDUCERS); 2015 Jun 21-25; Anchorage, USA. IEEE; 2015. pp. 1711-4. DOI
 104. Pothof F, Anees S, Leupold J, et al. Fabrication and characterization of a high-resolution neural probe for stereoelectroencephalography and single neuron recording. In: 2014 36th Annual International Conference of the IEEE Engineering in Medicine and Biology Society; 2014 Aug 26-30; Chicago, USA. IEEE; 2014. pp. 5244-7. DOI
 105. Schwaerzle M, Pothof F, Paul O, Ruther P. High-resolution optrode with integrated light source for deeper brain regions. *Procedia Eng* 2015;120:924-7. DOI
 106. Mekaru H, Takagi H, Ohtomo A, Kokubo M, Goto H. Soft patterning on cylindrical surface of plastic optical fiber. *J Vac Sci Technol B* 2011;29:06FC07. DOI
 107. Mekaru H, Ohtomo A, Takagi H, Kokubo M, Goto H. High-speed imprinting on plastic optical fibers using cylindrical mold with hybrid microstructures. *Microelect Eng* 2013;110:156-62. DOI
 108. Ding Y, Jiang J, Wu Y, et al. Porous conductive textiles for wearable electronics. *Chem Rev* 2024;124:1535-648. DOI
 109. Sadri B, Gao W. Fibrous wearable and implantable bioelectronics. *Appl Phys Rev* 2023;10:031303. DOI PubMed PMC
 110. Zhou S, Li J, Zhang Q, et al. Recent advance on fiber optic SPR/LSPR-based ultra-sensitive biosensors using novel structures and emerging signal amplification strategies. *Opt Laser Technol* 2024;175:110783. DOI
 111. Guo J, Zhou B, Yang C, Dai Q, Kong L. Stretchable and temperature-sensitive polymer optical fibers for wearable health monitoring. *Adv Funct Mater* 2019;29:1902898. DOI
 112. Abdelaziz MEMK, Zhao J, Gil Rosa B, et al. Fiberbots: robotic fibers for high-precision minimally invasive surgery. *Sci Adv* 2024;10:eadj1984. DOI PubMed PMC
 113. Park J, Sempionatto JR, Kim J, et al. Microscale biosensor array based on flexible polymeric platform toward lab-on-a-needle: real-time multiparameter biomedical assays on curved needle surfaces. *ACS Sens* 2020;5:1363-73. DOI
 114. Lin R, Jin Y, Li RR, et al. Needle-integrated ultrathin bioimpedance microsensor array for early detection of extravasation. *Biosens Bioelectron* 2022;216:114651. DOI
 115. Liu Z, Yu X, Huang J, Wu X, Wang Z, Zhu B. A review: flexible devices for nerve stimulation. *Soft Sci* 2024;4:4. DOI
 116. Vazquez R, Motovilova E, Winkler SA. Stretchable sensor materials applicable to radiofrequency coil design in magnetic resonance imaging: a review. *Sensors* 2024;24:3390. DOI PubMed PMC
 117. Yaras YS, Yildirim DK, Herzka DA, et al. Real-time device tracking under MRI using an acousto-optic active marker. *Magn Reson Med* 2021;85:2904-14. DOI PubMed PMC
 118. Jin J, Wang S, Zhang Z, Mei D, Wang Y. Progress on flexible tactile sensors in robotic applications on objects properties recognition, manipulation and human-machine interactions. *Soft Sci* 2023;3:8. DOI
 119. Sun G, Wang P, Jiang Y, Sun H, Meng C, Guo S. Recent advances in flexible and soft gel-based pressure sensors. *Soft Sci* 2022;2:17. DOI
 120. Kim J, Kim H, Lee M, et al. Progresses and perspectives of 1D soft sensing devices for healthcare applications. *Adv Funct Mater* 2024;34:2406651. DOI
 121. Duan S, Shi Q, Hong J, et al. Water-modulated biomimetic hyper-attribute-gel electronic skin for robotics and skin-attachable wearables. *ACS Nano* ;2023:1355-71. DOI
 122. Zhu P, Li Z, Pang J, He P, Zhang S. Latest developments and trends in electronic skin devices. *Soft Sci* 2024;4:17. DOI
 123. Kim KH, Kim JH, Ko YJ, Lee HE. Body-attachable multifunctional electronic skins for bio-signal monitoring and therapeutic applications. *Soft Sci* 2024;4:24. DOI
 124. Gao W, Huang J, He J, et al. Recent advances in ultrathin materials and their applications in e-skin. *InfoMat* 2023;5:e12426. DOI
 125. Hao Y, Yan Q, Liu H, et al. A stretchable, breathable, and self-adhesive electronic skin with multimodal sensing capabilities for human-centered healthcare. *Adv Funct Mater* 2023;33:2303881. DOI
 126. Yang JC, Mun J, Kwon SY, Park S, Bao Z, Park S. Electronic skin: recent progress and future prospects for skin-attachable devices for health monitoring, robotics, and prosthetics. *Adv Mater* 2019;31:e1904765. DOI PubMed
 127. Mi Q, Dong Y, Ge D, et al. Scalable manufacture of efficient, highly stable, and compact 3D imitation skin-based elastic triboelectric nanogenerator for energy harvesting and self-powered sensing. *Nano Energy* 2024;131:110283. DOI
 128. Ge D, Mi Q, Gong R, et al. Mass-producible 3D hair structure-editable silk-based electronic skin for multisenario signal monitoring and emergency alarming system. *Adv Funct Mater* 2023;33:2305328. DOI
 129. Lai Y, Ye B, Lu C, et al. Extraordinarily sensitive and low-voltage operational cloth-based electronic skin for wearable sensing and multifunctional integration uses: a tactile-induced insulating-to-conducting transition. *Adv Funct Mater* 2016;26:1286-95. DOI
 130. Jiang L, Yuan L, Wang W, Zhang Q. Soft materials for wearable supercapacitors. *Soft Sci* 2021;1:5. DOI

131. Yan C, Wang J, Kang W, et al. Highly stretchable piezoresistive graphene-nanocellulose nanopaper for strain sensors. *Adv Mater* 2014;26:2022-7. DOI PubMed
132. Geng W, Cuthbert TJ, Menon C. Conductive thermoplastic elastomer composite capacitive strain sensors and their application in a wearable device for quantitative joint angle prediction. *ACS Appl Polym Mater* 2021;3:122-9. DOI
133. Zhou J, Gu Y, Fei P, et al. Flexible piezotronic strain sensor. *Nano Lett* 2008;8:3035-40. DOI
134. Shuai L, Guo ZH, Zhang P, Wan J, Pu X, Wang ZL. Stretchable, self-healing, conductive hydrogel fibers for strain sensing and triboelectric energy-harvesting smart textiles. *Nano Energy* 2020;78:105389. DOI
135. Dong L, Gang T, Bian C, Tong R, Wang J, Hu M. A high sensitivity optical fiber strain sensor based on hollow core tapering. *Opt Fiber Technol* 2020;56:102179. DOI
136. Liu S, Zhang W, He J, Lu Y, Wu Q, Xing M. Fabrication techniques and sensing mechanisms of textile-based strain sensors: from spatial 1D and 2D perspectives. *Adv Fiber Mater* 2024;6:36-67. DOI
137. Li L, Xiang H, Xiong Y, et al. Ultrastretchable fiber sensor with high sensitivity in whole workable range for wearable electronics and implantable medicine. *Adv Sci* 2018;5:1800558. DOI PubMed PMC
138. Zhang J, Xu B, Chen K, Li Y, Li G, Liu Z. Revolutionizing digital healthcare networks with wearable strain sensors using sustainable fibers. *SusMat* 2024;4:e207. DOI
139. Wei X, Liang X, Meng C, Cao S, Shi Q, Wu J. Multimodal electronic textiles for intelligent human-machine interfaces. *Soft Sci* 2023;3:17. DOI
140. Sheng F, Zhang B, Zhang Y, et al. Ultrastretchable organogel/silicone fiber-helical sensors for self-powered implantable ligament strain monitoring. *ACS Nano* 2022;16:10958-67. DOI
141. Ning C, Cheng R, Jiang Y, et al. Helical fiber strain sensors based on triboelectric nanogenerators for self-powered human respiratory monitoring. *ACS Nano* 2022;16:2811-21. DOI
142. Zhou Z, Chen K, Li X, et al. Sign-to-speech translation using machine-learning-assisted stretchable sensor arrays. *Nat Electron* 2020;3:571-8. DOI
143. Frutiger A, Muth JT, Vogt DM, et al. Capacitive soft strain sensors via multicore-shell fiber printing. *Adv Mater* 2015;27:2440-6. DOI
144. Lee J, Ihle SJ, Pellegrino GS, et al. Stretchable and suturable fibre sensors for wireless monitoring of connective tissue strain. *Nat Electron* 2021;4:291-301. DOI
145. Tu J, Wang M, Li W, et al. Electronic skins with multimodal sensing and perception. *Soft Sci* 2023;3:24. DOI
146. Lan L, Zhao F, Yao Y, Ping J, Ying Y. One-step and spontaneous in situ growth of popcorn-like nanostructures on stretchable double-twisted fiber for ultrasensitive textile pressure sensor. *ACS Appl Mater Interfaces* 2020;12:10689-96. DOI PubMed
147. Jiang X, Ren Z, Fu Y, et al. Highly compressible and sensitive pressure sensor under large strain based on 3D porous reduced graphene oxide fiber fabrics in wide compression strains. *ACS Appl Mater Interfaces* 2019;11:37051-9. DOI
148. Lan L, Jiang C, Yao Y, Ping J, Ying Y. A stretchable and conductive fiber for multifunctional sensing and energy harvesting. *Nano Energy* 2021;84:105954. DOI
149. Chhetry A, Yoon H, Park JY. A flexible and highly sensitive capacitive pressure sensor based on conductive fibers with a microporous dielectric for wearable electronics. *J Mater Chem C* 2017;5:10068-76. DOI
150. Chen Y, Wang Z, Xu R, Wang W, Yu D. A highly sensitive and wearable pressure sensor based on conductive polyacrylonitrile nanofibrous membrane via electroless silver plating. *Chem Eng J* 2020;394:124960. DOI
151. Fan W, He Q, Meng K, et al. Machine-knitted washable sensor array textile for precise epidermal physiological signal monitoring. *Sci Adv* 2020;6:eaay2840. DOI PubMed PMC
152. Wang Y, Zhu M, Wei X, Yu J, Li Z, Ding B. A dual-mode electronic skin textile for pressure and temperature sensing. *Chem Eng J* 2021;425:130599. DOI
153. Fan W, Liu T, Wu F, et al. An antisweat interference and highly sensitive temperature sensor based on poly(3,4-ethylenedioxythiophene)-poly(styrenesulfonate) fiber coated with polyurethane/graphene for real-time monitoring of body temperature. *ACS Nano* 2023;17:21073-82. DOI PubMed PMC
154. Yun J. Recent progress in thermal management for flexible/wearable devices. *Soft Sci* 2023;3:12. DOI
155. Wang W, Yao D, Wang H, et al. A breathable, stretchable, and self-calibrated multimodal electronic skin based on hydrogel microstructures for wireless wearables. *Adv Funct Mater* 2024;34:2316339. DOI
156. Li Q, Zhang LN, Tao XM, Ding X. Review of flexible temperature sensing networks for wearable physiological monitoring. *Adv Healthc Mater* 2017;6:1601371. DOI PubMed
157. Husain M, Kennon R. Preliminary investigations into the development of textile based temperature sensor for healthcare applications. *Fibers* 2013;1:2-10. DOI
158. Kumar SRS, Kurra N, Alshareef HN. Enhanced high temperature thermoelectric response of sulphuric acid treated conducting polymer thin films. *J Mater Chem C* 2016;4:215-21. DOI
159. Lee J, Kim DW, Chun S, et al. Intrinsically strain-insensitive, hyperelastic temperature-sensing fiber with compressed micro-wrinkles for integrated textronics. *Adv Mater Technol* 2020;5:2000073. DOI
160. Li F, Xue H, Lin X, Zhao H, Zhang T. Wearable temperature sensor with high resolution for skin temperature monitoring. *ACS Appl Mater Interfaces* 2022;14:43844-52. DOI
161. Trung TQ, Le HS, Dang TML, Ju S, Park SY, Lee NE. Freestanding, fiber-based, wearable temperature sensor with tunable thermal

- index for healthcare monitoring. *Adv Healthc Mater* 2018;7:e1800074. DOI PubMed
162. Trung TQ, Dang TML, Ramasundaram S, Toi PT, Park SY, Lee NE. A stretchable strain-insensitive temperature sensor based on free-standing elastomeric composite fibers for on-body monitoring of skin temperature. *ACS Appl Mater Interfaces* 2019;11:2317-27. DOI PubMed
163. Afroj S, Karim N, Wang Z, et al. Engineering graphene flakes for wearable textile sensors via highly scalable and ultrafast yarn dyeing technique. *ACS Nano* 2019;13:3847-57. DOI PubMed PMC
164. Bubnova O, Khan ZU, Wang H, et al. Semi-metallic polymers. *Nat Mater* 2014;13:190-4. DOI
165. Ryu WM, Lee Y, Son Y, Park G, Park S. Thermally drawn multi-material fibers based on polymer nanocomposite for continuous temperature sensing. *Adv Fiber Mater* 2023;5:1712-24. DOI
166. Wang Z, Zhang L, Liu J, Li C. A flexible bimodal sensor based on an electrospun nanofibrous structure for simultaneous pressure-temperature detection. *Nanoscale* 2019;11:14242-9. DOI PubMed
167. Zhao X, Wang LY, Tang CY, et al. Smart Ti₃C₂T_x MXene fabric with fast humidity response and joule heating for healthcare and medical therapy applications. *ACS Nano* 2020;14:8793-805. DOI PubMed
168. Hu X, Quan B, Zhu C, et al. Upgrading electricity generation and electromagnetic interference shielding efficiency via phase-change feedback and simple origami strategy. *Adv Sci* 2023;10:e2206835. DOI PubMed PMC
169. Tan C, Cao X, Wu XJ, et al. Recent advances in ultrathin two-dimensional nanomaterials. *Chem Rev* 2017;117:6225-331. DOI
170. Cheng Y, Zhang H, Wang R, et al. Highly stretchable and conductive copper nanowire based fibers with hierarchical structure for wearable heaters. *ACS Appl Mater Interfaces* 2016;8:32925-33. DOI
171. Li Y, Liu X, Wang S, et al. Dopamine-induced high fiber wetness for improved conductive fiber bundles with striated polypyrrole coating toward wearable healthcare electronics. *Chem Eng J* 2024;485:149888. DOI
172. Villatoro E, Loyez M, Villatoro J, Caucheteur C, Albert J. Dual-mode comb plasmonic optical fiber sensing. *ACS Sens* 2024;9:3027-36. DOI PubMed PMC
173. Qian Y, Wang Q, Zhang D, Wang Y, Li B, Wang H. A high-performance long-range surface plasmon resonance sensor based on the co-modification of carbon nanotubes and gold nanorods. *Opt Fiber Technol* 2023;80:103460. DOI
174. Viegas D, Goicoechea J, Santos JL, et al. Sensitivity improvement of a humidity sensor based on silica nanospheres on a long-period fiber grating. *Sensors* 2009;9:519-27. DOI PubMed PMC
175. Fenjan DA, Mahdi BR, Yusr HA. Graphene oxide-coated mach-zehnder interferometer based ammonia gas sensor. *Nexo Rev Cient* 2024;36:1132-40. DOI
176. Zhang S, Han B, Zhang Y, Liu Y, Zheng W, Zhao Y. Multichannel fiber optic SPR sensors: realization methods, application status, and future prospects. *Laser Photonics Rev* 2022;16:2200009. DOI
177. Li Z, Xiao Y, Liu F, et al. Operando optical fiber monitoring of nanoscale and fast temperature changes during photo-electrocatalytic reactions. *Light Sci Appl* 2022;11:220. DOI PubMed PMC
178. Wang Q, Yin X, Yin P, et al. Research progress of resonance optical fiber sensors modified by low-dimensional materials. *Laser Photonics Rev* 2023;17:2200859. DOI
179. Ning W, Hu S, Zhou C, et al. An ultrasensitive J-shaped optical fiber LSPR aptasensor for the detection of *Helicobacter pylori*. *Anal Chim Acta* 2023;1278:341733. DOI
180. Pathak A, Gupta BD. Ultra-selective fiber optic SPR platform for the sensing of dopamine in synthetic cerebrospinal fluid incorporating permselective nafion membrane and surface imprinted MWCNTs-PPy matrix. *Biosens Bioelectron* 2019;133:205-14. DOI PubMed
181. Gomez D, Morgan SP, Hayes-gill BR, Correia RG, Korposh S. Polymeric optical fibre sensor coated by SiO₂ nanoparticles for humidity sensing in the skin microenvironment. *Sensor Actuat B Chem* 2018;254:887-95. DOI
182. Jain S, Paliwal A, Gupta V, Tomar M. Smartphone integrated handheld long range surface plasmon resonance based fiber-optic biosensor with tunable SiO₂ sensing matrix. *Biosens Bioelectron* 2022;201:113919. DOI PubMed
183. Samavati Z, Samavati A, Ismail AF, Othman MHD, Rahman MA. Comprehensive investigation of evanescent wave optical fiber refractive index sensor coated with ZnO nanoparticles. *Opt Fiber Technol* 2019;52:101976. DOI
184. Chauhan M, Singh VK. ZnO nanostructures coated no-core fiber refractive index sensor. *Mat Sci Semicon Proc* 2022;147:106757. DOI
185. Yin Z, Jing X, Li K, Zhang Z, Li J. Modulation of the sensing bandwidth of dual-channel SPR sensors by TiO₂ film. *Opt Laser Technol* 2024;169:110105. DOI
186. Imas JJ, Albert J, Villar ID, Ozcariz A, Zamarreno CR, Matias IR. Mode transitions and thickness measurements during deposition of nanoscale TiO₂ coatings on tilted fiber bragg gratings. *J Lightwave Technol* 2022;40:6006-12. DOI
187. Imas JJ, Matias IR, Del Villar I, Ozcariz A, Zamarreno CR, Albert J. All-fiber ellipsometer for nanoscale dielectric coatings. *Opto Electron Adv* 2023;10:230048. DOI
188. Sangeetha M, Madhan D. Ultra sensitive molybdenum disulfide (MoS₂)/graphene based hybrid sensor for the detection of NO₂ and formaldehyde gases by fiber optic clad modified method. *Opt Laser Technol* 2020;127:106193. DOI
189. Li X, Gong P, Zhou X, et al. In-situ detection scheme for EGFR gene with temperature and pH compensation using a triple-channel optical fiber biosensor. *Anal Chim Acta* 2023;1263:341286. DOI
190. Wang Q, Wang X, Song H, Zhao W, Jing J. A dual channel self-compensation optical fiber biosensor based on coupling of surface plasmon polariton. *Opt Laser Technol* 2020;124:106002. DOI

191. Siyu E, Zhang Y, Han B, Zheng W, Wu Q, Zheng H. Two-channel surface plasmon resonance sensor for simultaneous measurement of seawater salinity and temperature. *IEEE Trans Instrum Meas* 2020;69:7191-9. [DOI](#)
192. Zheng W, Han B, Zhang YN, Liu L, Zhao Y. An in-fiber sensor for simultaneous measurement of cholesterol concentration and temperature based on SPR and MMI. *Anal Chim Acta* 2024;1287:342043. [DOI](#)
193. Xiang S, You H, Miao X, et al. An ultra-sensitive multi-functional optical micro/nanofiber based on stretchable encapsulation. *Sensors* 2021;21:7437. [DOI PubMed PMC](#)
194. Chen M, He Y, Liang H, et al. Stretchable and strain-decoupled fluorescent optical fiber sensor for body temperature and movement monitoring. *ACS Photonics* 2022;9:1415-24. [DOI](#)
195. Jiang Q, Liang X, Chen Z, et al. Wearable strain sensor integrating mechanoluminescent fiber with a flexible printed circuit. *Opt Lett* 2024;49:1221-4. [DOI](#)
196. Guo J, Zhou B, Yang C, Dai Q, Kong L. Stretchable and upconversion-luminescent polymeric optical sensor for wearable multifunctional sensing. *Opt Lett* 2019;44:5747-50. [DOI](#)
197. Quandt BM, Braun F, Ferrario D, et al. Body-monitoring with photonic textiles: a reflective heartbeat sensor based on polymer optical fibres. *J R Soc Interface* 2017;14:20170060. [DOI PubMed PMC](#)
198. Schiff H, Halbeisen M, Schütz U, Delafoche B, Vogelsang K, Gobrecht J. Surface structuring of textile fibers using roll embossing. *Microelect Eng* 2006;83:855-8. [DOI](#)
199. Dai M, de Jong TM, Sánchez C, et al. Surface structuring of bi-component fibres with photoembossing. *RSC Adv* 2012;2:9964. [DOI](#)
200. Mekaru H, Ohtomo A, Takagi H. Effect of buffer materials on thermal imprint on plastic optical fiber. *Microsyst Technol* 2013;19:325-33. [DOI](#)
201. Wang S, Wang X, Wang Q, et al. Flexible optoelectronic multimodal proximity/pressure/temperature sensors with low signal interference. *Adv Mater* 2023;35:e2304701. [DOI](#)
202. Mekaru H, Ohtomo A, Takagi H, Kokubo M, Goto H. Development of reel-to-reel process system for roller-imprint on plastic fibers. *Microelect Eng* 2011;88:2059-62. [DOI](#)
203. Yu C, Chen H. Nanoimprint technology for patterning functional materials and its applications. *Microelect Eng* 2015;132:98-119. [DOI](#)
204. Kooy N, Mohamed K, Pin LT, Guan OS. A review of roll-to-roll nanoimprint lithography. *Nanoscale Res Lett* 2014;9:320. [DOI PubMed PMC](#)
205. Ohtomo A, Kokubo M, Goto H, Mekaru H, Takagi H. Fast and continuous patterning on the surface of plastic fiber by using thermal roller imprint. *J Vac Sci Technol B* 2012;30:06FB01. [DOI](#)
206. Giovannini G, Sharma K, Boesel LF, Rossi RM. Lab-on-a-fiber wearable multi-sensor for monitoring wound healing. *Adv Healthc Mater* 2024;13:e2302603. [DOI PubMed](#)
207. Li Y, Wang P, Meng C, Chen W, Zhang L, Guo S. A brief review of miniature flexible and soft tactile sensors for interventional catheter applications. *Soft Sci* 2022;2:6. [DOI](#)
208. Park J, Choi WM, Kim K, Jeong WI, Seo JB, Park I. Biopsy needle integrated with electrical impedance sensing microelectrode array towards real-time needle guidance and tissue discrimination. *Sci Rep* 2018;8:264. [DOI PubMed PMC](#)
209. Mishra V, Schned AR, Hartov A, Heaney JA, Seigne J, Halter RJ. Electrical property sensing biopsy needle for prostate cancer detection. *Prostate* 2013;73:1603-13. [DOI PubMed](#)
210. Yu X, Wang H, Ning X, et al. Needle-shaped ultrathin piezoelectric microsystem for guided tissue targeting via mechanical sensing. *Nat Biomed Eng* 2018;2:165-72. [DOI](#)
211. Park J, Cha DI, Jeong Y, et al. Real-time internal steam pop detection during radiofrequency ablation with a radiofrequency ablation needle integrated with a temperature and pressure sensor: preclinical and clinical pilot tests. *Adv Sci* 2021;8:e2100725. [DOI PubMed PMC](#)
212. Jeong Y, Park J, Lee J, Kim K, Park I. Ultrathin, biocompatible, and flexible pressure sensor with a wide pressure range and its biomedical application. *ACS Sens* 2020;5:481-9. [DOI](#)
213. Park YL, Elayaperumal S, Daniel B, et al. Real-time estimation of 3-D needle shape and deflection for MRI-guided interventions. *IEEE ASME Trans Mechatron* 2010;15:906-15. [DOI PubMed PMC](#)
214. Zhou C, Yang Y, Wang J, et al. Ferromagnetic soft catheter robots for minimally invasive bioprinting. *Nat Commun* 2021;12:5072. [DOI PubMed PMC](#)
215. Chen R, Canales A, Anikeeva P. Neural recording and modulation technologies. *Nat Rev Mater* 2017;2:16093. [DOI PubMed PMC](#)
216. Pothof F, Galchev T, Patel M, Herbawi AS, Paul O, Ruther P. Heterogeneous integration of analog CMOS chips on flexible substrates for high-resolution deep brain epilepsy diagnosis. *Procedia Eng* 2015;120:920-3. [DOI](#)
217. Raducanu BC, Yazicioglu RF, Lopez CM, et al. Time multiplexed active neural probe with 1356 parallel recording sites. *Sensors* 2017;17:2388. [DOI PubMed PMC](#)
218. Steinmetz NA, Aydin C, Lebedeva A, et al. Neuropixels 2.0: a miniaturized high-density probe for stable, long-term brain recordings. *Science* 2021;372:eabf4588. [DOI PubMed PMC](#)
219. Chen G, Xu S, Zhou Q, et al. Temperature-gated light-guiding hydrogel fiber for thermoregulation during optogenetic neuromodulation. *Adv Fiber Mater* 2023;5:968-78. [DOI](#)
220. Kim Y, Lee Y, Yoo J, et al. Multifunctional and flexible neural probe with thermally drawn fibers for bidirectional synaptic probing in the brain. *ACS Nano* 2024;18:13277-85. [DOI PubMed PMC](#)

221. Pu Z, Zhang X, Wu H, Wu J, Yu H, Li D. Cylindrical electrochemical sensor fabricated by rotated inkjet printing on flexible substrate for glucose monitoring. In: 2017 19th International Conference on Solid-State Sensors, Actuators and Microsystems (TRANSDUCERS); 2017 Jun 18-22; Kaohsiung, Taiwan. IEEE; 2017. pp. 1241-4. DOI
222. Marvin JS, Shimoda Y, Magloire V, et al. A genetically encoded fluorescent sensor for in vivo imaging of GABA. *Nat Methods* 2019;16:763-70. DOI
223. Krämer J, Kang R, Grimm LM, De Cola L, Picchetti P, Biedermann F. Molecular probes, chemosensors, and nanosensors for optical detection of biorelevant molecules and ions in aqueous media and biofluids. *Chem Rev* 2022;122:3459-636. DOI PubMed PMC
224. Musolino S, Schartner EP, Tsiminis G, Salem A, Monro TM, Hutchinson MR. Portable optical fiber probe for in vivo brain temperature measurements. *Biomed Opt Express* 2016;7:3069-77. DOI PubMed PMC
225. Shin J, Liu Z, Bai W, et al. Bioresorbable optical sensor systems for monitoring of intracranial pressure and temperature. *Sci Adv* 2019;5:eaaw1899. DOI PubMed PMC
226. Crane BC, Barwell NP, Gopal P, et al. The development of a continuous intravascular glucose monitoring sensor. *J Diabetes Sci Technol* 2015;9:751-61. DOI PubMed PMC
227. Forderhase AG, Ligons LA, Norwood E, McCarty GS, Sombers LA. Optimized fabrication of carbon-fiber microbiosensors for codetection of glucose and dopamine in brain tissue. *ACS Sens* 2024;9:2662-72. DOI PubMed
228. Nan K, Babae S, Chan WW, et al. Low-cost gastrointestinal manometry via silicone-liquid-metal pressure transducers resembling a quipu. *Nat Biomed Eng* 2022;6:1092-104. DOI PubMed
229. Nam S, Cha GD, Sunwoo SH, et al. Needle-like multifunctional biphasic microfiber for minimally invasive implantable bioelectronics. *Adv Mater* 2024;36:e2404101. DOI
230. Abdelaziz MEMK, Tian L, Hamady M, Yang G, Temelkuran B. X-ray to MR: the progress of flexible instruments for endovascular navigation. *Prog Biomed Eng* 2021;3:032004. DOI
231. Settecase F, Martin AJ, Lillaney P, Losey A, Hetsz SW. Magnetic resonance-guided passive catheter tracking for endovascular therapy. *Magn Reson Imaging Clin N Am* 2015;23:591-605. DOI PubMed PMC
232. Ratnayaka K, Faranesh AZ, Hansen MS, et al. Real-time MRI-guided right heart catheterization in adults using passive catheters. *Eur Heart J* 2013;34:380-9. DOI PubMed PMC
233. Ratnayaka K, Rogers T, Schenke WH, et al. Magnetic resonance imaging-guided transcatheter cavopulmonary shunt. *JACC Cardiovasc Interv* 2016;9:959-70. DOI PubMed PMC
234. Yildirim KD, Basar B, Campbell-Washburn AE, Herzka DA, Kocaturk O, Lederman RJ. A cardiovascular magnetic resonance (CMR) safe metal braided catheter design for interventional CMR at 1.5 T: freedom from radiofrequency induced heating and preserved mechanical performance. *J Cardiovasc Magn Reson* 2019;21:16. DOI PubMed PMC
235. Chubb H, Williams SE, Whitaker J, Harrison JL, Razavi R, O'Neill M. Cardiac electrophysiology under MRI guidance: an emerging technology. *Arrhythm Electrophysiol Rev* 2017;6:85-93. DOI PubMed PMC
236. Saikus CE, Ratnayaka K, Barbash IM, et al. MRI-guided vascular access with an active visualization needle. *J Magn Reson Imaging* 2011;34:1159-66. DOI PubMed PMC
237. Kaiser M, Detert M, Rube MA, et al. Resonant marker design and fabrication techniques for device visualization during interventional magnetic resonance imaging. *Biomed Tech* 2015;60:89-103. DOI
238. Su H, Kwok KW, Cleary K, et al. State of the art and future opportunities in MRI-guided robot-assisted surgery and interventions. *Proc IEEE Inst Electr Electron Eng* 2022;110:968-92. DOI PubMed PMC
239. Ellersiek D, Fassbender H, Bruners P, et al. A monolithically fabricated flexible resonant circuit for catheter tracking in magnetic resonance imaging. *Sensor Actuat B Chem* 2010;144:432-6. DOI